

SYNTHESIS AND CHARACTERIZATION OF A NEW SOLUBLE  
POLYTHIOPHENE DERIVATIVE AND ITS ELECTROCHROMIC  
APPLICATION

A THESIS SUBMITTED TO  
THE GRADUATE SCHOOL OF NATURAL AND APPLIED SCIENCES  
OF  
MIDDLE EAST TECHNICAL UNIVERSITY

BY

SİMGE TARKUÇ

IN PARTIAL FULFILLMENT OF THE REQUIREMENTS  
FOR  
THE DEGREE OF MASTER OF SCIENCE  
IN  
CHEMISTRY

DECEMBER 2006

Approval of the Graduate School of Natural and Applied Sciences

---

Prof. Dr. Canan Özgen  
Director

I certify that this thesis satisfies all the requirements as a thesis for the degree of Master of Sciences.

---

Prof. Dr. Ahmet M. Önal  
Head of Department

This is to certify that we have read this thesis and that in our opinion it is fully adequate, in scope and quality, as a thesis and for the degree of Master of Sciences.

---

Prof. Dr. Cihangir Tanyeli  
Co-Supervisor

---

Prof. Dr. Levent Toppare  
Supervisor

Examining Committee Members

Prof. Dr. Leyla Aras (METU, CHEM)

---

Prof. Dr. Levent Toppare (METU, CHEM)

---

Prof. Dr. Cihangir Tanyeli (METU, CHEM)

---

Prof. Dr. Mustafa Güllü (Ankara Univ, CHEM)

---

Asst. Prof. Dr. Erdal Onurhan (METU, CHEM)

---

**I hereby declare that all information in this document has been obtained and presented in accordance with academic rules and ethical conduct. I also declare that, as required by these rules and conduct, I have fully cited and referenced all material and results that are not original to this work.**

**Name, Last name:**

**Signature :**

## ABSTRACT

### SYNTHESIS AND CHARACTERIZATION OF A NEW SOLUBLE POLYTHIOPHENE DERIVATIVE AND ITS ELECTROCHROMIC APPLICATION

Tarkuç, Simge

M.S., Department of Chemistry

Supervisor: Prof. Dr. Levent Toppare

Co-Supervisor: Prof. Dr. Cihangir Tanyeli

December 2006, 89 pages

The Knorr-Paal reaction of 1,4-di(2-thienyl)-1,4-butanedione with aniline to yield 1-phenyl-2,5-di(2-thienyl)-1*H*-pyrrole (PTP) was performed in the presence of catalytical amounts of *p*-toluenesulfonic acid (PTSA). Chemical polymerization of the monomer yielded a soluble polymer. Structures of both the monomer and the polymer were investigated by Nuclear Magnetic Resonance (<sup>1</sup>H and <sup>13</sup>C NMR) and Fourier Transform Infrared (FTIR) Spectroscopy. The average molecular weight of the chemically synthesized polymer was determined by Gel Permeation Chromatography (GPC) as  $M_n = 7.2 \times 10^3$  g/mol. The electrochemical oxidative polymerization of PTP was carried out via potentiodynamic electrolysis in the presence of LiClO<sub>4</sub>, NaClO<sub>4</sub> (1:1) being the supporting electrolyte in acetonitrile. Electrochemical copolymerization of PTP with 3,4-ethylenedioxythiophene (EDOT) was carried out in acetonitrile (ACN)/ NaClO<sub>4</sub>/LiClO<sub>4</sub> (0.1M) solvent-electrolyte couple system via potentiodynamic electrolysis. Cyclic voltammetry was used

to investigate electrochemical behavior of the monomer and redox reactions of conducting polymers. Conductivities of films of the polymers were measured by four-probe technique. Surface morphologies of the films were investigated by Scanning Electron Microscope (SEM). Electrochromic properties of the conducting polymers were investigated via spectroelectrochemistry, kinetic and colorimetry studies. Spectroelectrochemical analysis of P(PTP) revealed electronic transitions at 413, 600 and 900 nm corresponding to  $\pi$ - $\pi^*$  transition, polaron, and bipolaron band formations, respectively. The spectroelectrochemical behavior of the P(PTP-co-EDOT) in comparison to those of the respective homopolymers revealed solid evidence of copolymerization based upon the differences in the spectral signatures. Switching time of the polymers was evaluated by kinetic studies upon measuring the percent transmittance (%T) at the maximum contrast point. As an application, absorption/transmission type electrochromic devices with ITO/homopolymer(copolymer)/gel electrolyte/PEDOT/ITO configuration was constructed, where homopolymer (copolymer) and PEDOT functioned as the anodically and the cathodically coloring layers, respectively. Spectroelectrochemistry, switching ability and open circuit memory of the devices were investigated. The results revealed that these devices have good switching times, reasonable contrasts and optical memories.

**Keywords:** Electropolymerization; Conducting polymers; Electrochromic properties; Electrochromic devices; Copolymerization

## ÖZ

### YENİ BİR ÇÖZÜNÜR POLİTİYOFEN TÜREVİNİN SENTEZİ, KARAKTERİZASYONU VE ELEKTROKROMİK CİHAZLARDA KULLANIMI

Tarkuç, Simge

Yüksek Lisans, Kimya Bölümü

Tez Yöneticisi: Prof. Dr. Levent Toppare

Ortak Tez Yöneticisi: Prof. Dr. Cihangir Tanyeli

Aralık 2006, 89 sayfa

1-Fenil-2,5-di(tiyofen-2-il)-1*H*-pirol (PTP); anilin ve 4-di(2-tiyenil)-1,4-butandion'un az miktarda p-toluensulfonik asit (PTSA) varlığında Knorr-Paal reaksiyonu ile sentezlenmiştir. PTP monomerinin kimyasal olarak polimerleştirilmesi sonucunda çözünür polimer elde edilmiştir. Monomer ile polimerin kimyasal yapıları <sup>1</sup>H, <sup>13</sup>C Nükleer Manyetik Rezonans (NMR) and Fourier Transform Infrared Spektroskopisi (FTIR) ile karakterize edilmiştir. Polimerin ortalama molekül ağırlığı Jel Geçirgenlik Kromatografisi (GPC) ile  $M_n = 7.2 \times 10^3$  gr/mol olarak belirlenmiştir. Monomerin elektrokimyasal polimerizasyonu LiClO<sub>4</sub>, NaClO<sub>4</sub> (1:1) destek elektrolitleri varlığında asetonitrilde gerçekleştirilmiştir. PTP'nin EDOT varlığındaki elektrokimyasal kopolimeri ACN/ NaClO<sub>4</sub>/ LiClO<sub>4</sub> (1:1) çözücü-elektrolit ikilisinde potensiyodinamik metotla sentezlenmiştir. Dönüşümlü Voltametre (CV) yöntemi ile monomerin elektrokimyasal davranışı ve iletken polimerlerin redox reaksiyonları belirlendi. Polimer filmlerinin iletkenlikleri dört nokta

tekniki ile ölçülmüştür. Taramalı Elektron Mikroskobu ile polimer filmlerinin morfolojisi incelenmiştir. Sentezlenen iletken polimerlerin elektrokromik özellikleri spektroeletrokimyasal, kinetik ve kolorimetrik çalışmalarla araştırılmıştır. Spektroeletrokimyasal analizler ile P(PTP)'nin elektronik geçişleri  $\pi$ - $\pi^*$  geçişi, polaron ve bipolaron bantlarının oluşumuna bağlı olarak sırasıyla 413, 600 ve 900 nm de gözlemlenmiştir. Spektroeletrokimyasal analizler sonucunda kopolimerin ,P(PTP-co-EDOT), her iki homopolimerden de farklı bir elektrokromik özelliğe sahip olduğu gösterilmiştir. Polimerlerin tepki zamanı yüzde transmittans ölçümlerinin de yapıldığı kinetik çalışmalarla en yüksek kontrast noktasında incelenmiştir. Soğurma/yansıtma tipi elektrokromik cihazlar ITO/ homopolimer veya kopolimer/ jel elektrolit/ PEDOT konfigürasyonunda kurulmuştur. Bu cihazlarda homopolimer (kopolimer) yükseltildiğinde, PEDOT ise indirildiğinde renklenmiş katman olarak kullanılmıştır. Bu cihazların spektroeletrokimya, tepki özellikleri, açık devre hafızaları araştırılmıştır. Cihazların uygun optik kontrastları ve açık devre hafızaları olduğu bulunmuştur.

**Anahtar sözcükler:** Elektrokimyasal polimerleşme; iletken polimerler; elektrokromik özellikler; elektrokromik cihazlar; kopolimerizasyon

***TO MY FAMILY***

## ACKNOWLEDGMENTS

I would like to express my sincere gratitude to the excellent and diligent guidance of Prof. Dr. Levent Toppare for his valuable suggestion, stimulating advice, creative and energetic instructions.

I would like to thank, Prof. Dr. İdris Mecidođlu Akhmedov and Prof. Dr. Cihangir Tanyeli for their valuable discussions.

I would like to express my special thanks to Dr. Ertuđrul Őahmetliođlu, Dr. Elif Őahin, Dr. Pınar Őamurlu, Dr. Senem Kıralp and Metin Ak for their endless helps, stimulating conversations besides their kind friendships.

Special thanks go to my dear friends BaŐak Yiđitsoy, Serhat VarıŐ, Gorkem GUnbaŐ, Ođlem TUrkarŐlan and Yusuf Nur for their friendship; useful conversations and cooperation. I also would like to thank all my lab-mates in our research group for their kind friendship.

Words fail to express my eternal gratitude to my parents for their unwavering support of my decision and my sister Sinem TarkuŐ , who has given me unending support and encouragement.

I would like to extend my deepest gratitude to Nurten Serger for her endless patience and encouragement through both undergraduate and graduate school.

Finally, I would like thank the Scientific and Technological Research Council of Turkey (TUBITAK) for financial support which enabled me to carry out this work.

## TABLE OF CONTENTS

ABSTRACT .....	iv
ÖZ .....	vi
ACKNOWLEDGMENTS.....	ix
TABLE OF CONTENTS .....	x
LIST OF FIGURES .....	xiii
LIST OF TABLES.....	xvi
ABBREVIATIONS .....	xvii
INTRODUCTION .....	1
1.1. Conducting Polymers .....	1
1.1.1. Brief History of Conducting Polymers.....	1
1.2. Band Theory and Conduction Mechanism in Conducting Polymers.....	3
1.2.1. Band Theory.....	4
1.2.2. Conduction Mechanism .....	7
1.2.2.1. Charge Carriers.....	7
1.2.2.2. Concept of Doping.....	9
1.2.2.3. Hopping.....	13
1.3. Synthesis of Conducting Polymers .....	15
1.3.1. Chemical Polymerization.....	16
1.3.2. Electrochemical Polymerization .....	17
1.3.2.1. Mechanism of Electrochemical Polymerization.....	19
1.3.2.2. Effects of Electrolytic Conditions .....	20
1.3.2.3. Monomer Structure and Substituent Effects in Electropolymerization .....	22
1.4. Conducting Copolymers .....	26
1.5. Characterization of Conducting Polymers.....	26
1.6. Applications of Conducting Polymers .....	27

1.7. Chromism .....	28
1.7.1. Electrochromism .....	28
1.7.2. Types of Electrochromic Materials .....	30
1.7.3. Spectroelectrochemistry .....	31
1.8. Electrochromic Devices (ECD) .....	31
1.9. Characteristics of Electrochromic Device .....	33
1.9.1. Electrochromic Contrast and Switching Speed .....	33
1.9.2. Open Circuit Memory and Stability .....	34
1.9.3. Colorimetry .....	34
1.10. Aims of the Work .....	36
EXPERIMENTAL .....	37
2.1. Materials .....	37
2.2. Equipment .....	37
2.3. Procedure .....	38
2.3.1. Synthesis of monomer .....	38
2.3.1.1. Synthesis of 1,4-di(2-thienyl)-1,4-butanedione (I) .....	38
2.3.1.2. Synthesis of 1-Phenyl-2,5-di(2-thienyl)-1H-pyrrole (II) .....	39
2.4. Synthesis of Conducting Polymers .....	40
2.4.1. Electrochemical Polymerization .....	40
2.4.1.1. Synthesis of Homopolymer of PTP .....	40
2.4.1.2. Synthesis of Copolymer of PTP with 3,4-Ethylenedioxythiophene (EDOT) .....	41
2.4.2. Chemical Polymerization .....	42
2.5. Characterization of Conducting Polymers .....	42
2.5.1. Cyclic Voltammetry (CV) .....	42
2.5.2. Conductivity Measurements .....	45
2.5.3. Gel Permeation Chromatography (GPC) .....	46
2.5.4. Scanning Electron Microscope (SEM) .....	46
2.5.5. Electrochromic Properties of Conducting Polymers .....	47
2.5.5.1. Spectroelectrochemical Studies .....	47
2.5.5.2. Switching Studies .....	48

2.5.5.3. Colorimetry .....	49
2.6. Electrochromic Device (ECD) Construction .....	49
2.6.1. P(PTP)/PEDOT Electrochromic Device.....	49
2.6.2. P(PTP-co-EDOT)/PEDOT.....	50
2.6.3. Preparation of Gel Electrolyte.....	51
2.7. Characterization of Electrochromic Devices .....	51
2.7.1. Spectroelectrochemistry Studies of Electrochromic Devices .....	51
2.7.2. Switching Properties of Electrochromic Devices.....	52
2.7.3. Stability of Electrochromic Devices.....	52
2.7.4. Open Circuit Memory .....	52
RESULTS AND DISCUSSION.....	54
3.1. Characterization by <sup>1</sup> H-NMR and <sup>13</sup> C- NMR Spectroscopy .....	54
3.2. FTIR Spectra.....	56
3.3. Cyclic Voltammograms.....	59
3.4. Conductivities of the films .....	61
3.5. Morphologies of the films .....	61
3.6. Gel Permeation Chromatography (GPC).....	62
3.7. Investigation of Electrochromic Properties of Polymers .....	63
3.7.1. Spectroelectrochemistry .....	63
3.7.2. Electrochromic Switching.....	66
3.8. Characterization of Electrochromic Devices (ECDs) .....	70
3.8.1. Spectroelectrochemistry of ECDs .....	70
3.8.2 Switching of ECDs .....	73
3.8.3. Open Circuit Memory .....	75
3.8.4. Stability of ECDs.....	77
CONCLUSION .....	79
REFERENCES .....	81

## LIST OF FIGURES

<b>Figure 1.1</b> Common conducting polymer structures: (a) polyacetylene, (b) polythiophene, (c) polyfuran, (d) polypyrrole, (e) polyphenylene, (f) polyaniline, (g) polycarbazole .....	2
<b>Figure 1.2</b> Conjugated polymer structure (a) cis-polyacetylene and (b) polythiophene .....	4
<b>Figure 1.3</b> Band structure in an electronically conducting polymer.....	5
<b>Figure 1.4</b> Band structure for (a) a metal (b) a semiconductor and (c) an insulator.....	6
<b>Figure 1.5</b> Generation of bands in conjugated polymer systems.....	7
<b>Figure 1.6</b> Structural changes in polythiophene upon doping with a suitable oxidant.....	8
<b>Figure 1.7</b> Reversible doping-dedoping process of polythiophene .....	9
<b>Figure 1.8</b> Band model of (a) non-doped, (b) slightly doped, and (c) heavily doped conducting polymers .....	11
<b>Figure 1.9</b> Schematic illustration of doping (a) p-doping and (b) n-doping of conducting polymers [27] .....	12
<b>Figure 1.10</b> Conductivities of some metals, semiconductors and insulators ...	13
<b>Figure 1.11</b> Charge carrier transport in a conducting polymer .....	14
<b>Figure 1.12</b> Oxidative chemical polymerization of pyrrole in the presence of iron (III) chloride .....	16
<b>Figure 1.13</b> Chemical polymerization of polythiophene in the presence of metal-catalyze.....	17
<b>Figure 1.14</b> Electrochemical synthetic routes to polythiophene .....	18
<b>Figure 1.15</b> Proposed mechanisms for the electropolymerization of thiophene .....	20

<b>Figure 1.16</b> Absorption spectra of PTh and a few alkyl derivatives of 3-substituted PThs: (---) PTh; (— — —) P3MTh; (— . — .) P3BTh; (— —) P3HTh .....	23
<b>Figure 1.17</b> Competitive reaction pathways in unsubstituted polythiophene ..	24
<b>Figure 1.18</b> Polaron and bipolaron in non-degenerate ground state polymers: band diagrams for neutral (a), positive polaron (b) and positive bipolaron (c)	29
<b>Figure 1.19</b> Schematic illustrations of dual type electrochromic device .....	32
<b>Figure 1.20</b> Schematic representations of dual type (a) reflective and (b) transmissive type electrochromic device configurations [79].....	33
<b>Figure 1.21</b> CIE LAB color space .....	35
<b>Figure 2.1</b> (a) Triangular wave form (b) A cyclic voltammogram for a reversible redox reaction.....	43
<b>Figure 2.2</b> Cyclic voltammetry cell .....	44
<b>Figure 2.3</b> Four-probe conductivity measurement setup [93] .....	45
<b>Figure 2.4</b> In-situ optoelectrochemical analysis.....	47
<b>Figure 2.5</b> Square wave voltammetry .....	48
<b>Figure 2.6</b> Schematic illustration of dual type absorptive/transmissive type P(PTP)/PEDOT ECD configuration .....	50
<b>Figure 3.1</b> <sup>1</sup> H-NMR spectrum of PTP.....	55
<b>Figure 3.2</b> <sup>13</sup> C-NMR spectrum of PTP.....	55
<b>Figure 3.3</b> <sup>1</sup> H-NMR spectrum of the chemically synthesized P(PTP).....	56
<b>Figure 3.4</b> FTIR spectra of (a) PTP, (b) electrochemically synthesized P(PTP), and (c) chemically synthesized P(PTP) .....	57
<b>Figure 3.5</b> FTIR spectrum of P(PTP-co-EDOT) .....	58
<b>Figure 3.6</b> Cyclic voltammogram of P(PTP).....	59
<b>Figure 3.7</b> Cyclic voltammograms of (a) P(PTP-co-EDOT), (b) pristine PEDOT .....	60
<b>Figure 3.8</b> SEM micrographs of (a) P(PTP), (b) P(PTP-co-EDOT) (c) PEDOT .....	62
<b>Figure 3.9</b> Spectroelectrochemical spectrum of P(PTP) with applied potentials between -0.2 V and + 1.0 V in ACN/NaClO <sub>4</sub> /LiClO <sub>4</sub> (0.1 M) .....	64

<b>Figure 3.10</b> Polaron and bipolarons in non-degenerate ground state P(PTP): band diagrams for (a) neutral , (b) polaron and (c) bipolaron.....	65
<b>Figure 3.11</b> Spectroelectrochemical spectrum of P(PTP-co-EDOT) with applied potentials between -0.5 V and +1.2 V in ACN/NaClO <sub>4</sub> /LiClO <sub>4</sub> (0.1 M) .....	66
<b>Figure 3.12</b> Electrochromic switching, optical absorbance change monitored at 418 nm for P(PTP) between -0.2 V and + 1.0 V .....	67
<b>Figure 3.13</b> Electrochromic switching, optical absorbance change monitored at 480 nm for P(PTP-co-EDOT) between -0.5V and +1.2 V.....	68
<b>Figure 3.14</b> Spectroelectrochemical spectrum of P(PTP)/PEDOT device with applied potentials between -0.6 and +1.6 V .....	71
<b>Figure 3.15</b> Spectroelectrochemical spectrum of P(PTP-co-EDOT)/PEDOT device with applied potentials between -0.8 and +1.8 V .....	72
<b>Figure 3.16</b> Electrochromic switching, optical absorbance change monitored at 386 nm for P(PTP)/PEDOT device between -0.6 V and 1.6 V.....	73
<b>Figure 3.17</b> Electrochromic switching, optical absorbance change monitored at 545 nm for P(PTP-co-EDOT)/PEDOT device between -0.8 V and 1.8 V .....	74
<b>Figure 3.18</b> Open circuit memory of P(PTP-co-EDOT)/PEDOT device monitored at -0.6 V and +1.6 V potentials were applied for one second for each 200 seconds time interval at 386 nm .....	76
<b>Figure 3.19</b> Open circuit memory of P(PTP-co-EDOT)/PEDOT device monitored at -0.8 V and +1.8 V potentials were applied for one second for each 200 seconds time interval at 545 nm .....	76
<b>Figure 3.20</b> Stability test of P(PTP)/PEDOT device via cyclic voltammetry with a scan rate of 500 mV.s <sup>-1</sup> .....	78
<b>Figure 3.21</b> Stability test of P(PTP-co-EDOT)/PEDOT device via cyclic voltammetry with a scan rate of 500 mV.s <sup>-1</sup> .....	78

## LIST OF TABLES

<b>Table 1.1</b> Electrochromic properties of thiophene derivatives	25
<b>Table 3.1</b> Conductivities of Films of Polymers ( $\text{S}\cdot\text{cm}^{-1}$ )	61
<b>Table 3.2</b> GPC Results	63
<b>Table 3.3</b> Electrochromic properties of P(PTP)	69
<b>Table 3.4</b> Electrochromic properties of P(PTP-co-EDOT)	69
<b>Table 3.5</b> Colorimetry data for P(PTP)/PEDOT and P(PTP-co-EDOT)/PEDOT ECDs	72

## ABBREVIATIONS

PTP	1-Phenyl-2,5-di(2-thienyl)-1 <i>H</i> -pyrrole
P(PTP)	Poly(1-phenyl-2,5-di(2-thienyl)-1 <i>H</i> -pyrrole)
EDOT	3,4-Ethylenedioxythiophene
P(PTP-co-EDOT)	Poly(1-phenyl-2,5-di(2-thienyl)-1 <i>H</i> -pyrrole-co-ethylenedioxythiophene)
Th	Thiophene
Py	Pyrrole
PEDOT	Poly(3,4-ethylenedioxythiophene)
ACN	Acetonitrile
TBAFB	Tetrabutylammonium tetrafluoroborate
PMMA	Poly(methylmethacrylate)
PC	Propylene carbonate
NMR	Nuclear Magnetic Resonance
FTIR	Fourier Transform Infrared Spectrometer
CV	Cyclic Voltammetry
SEM	Scanning Electron Microscopy
GPC	Gel Permeation Chromatography
ECD	Electrochromic Device
HOMO	Highest Occupied Molecular Orbital
LUMO	Lowest Unoccupied Molecular Orbital
$E_g$	Band Gap Energy
CIE	La Commission Internationale de l'Eclairage
L a b	Luminance, hue, saturation

# CHAPTER I

## INTRODUCTION

### 1.1. Conducting Polymers

The discovery by MacDiarmid, Shirakawa, Heeger and co-workers that the conductivity of polyacetylene (PAC) could be increased by more than eleven orders of magnitude upon doping with iodine [1] led to great interest in conducting polymers and to the award of the 2000 Nobel Prize for Chemistry to these researchers. Then a new class of organic polymers, conducting polymers, with the remarkable ability to conduct an electrical current began to promote tremendous technological and scientific interest.

#### 1.1.1. Brief History of Conducting Polymers

Conventional polymers have been used for many applications traditionally because of their attractive chemical, mechanical, and electrically insulating properties [2].

The idea that conjugated polymers could be good electrical conductors has roots back to the 1960s when MacDiarmid and others discovered that poly(sulfurnitride)  $(\text{SN})_x$ , a polymeric inorganic explosive, has a high conductivity. The interesting electrical properties of  $(\text{SN})_x$  represented a step toward conducting polymers as they are known today [3,4].

The first electrochemical synthesis of a conducting polymer was reported by Letheby in 1862. The anodic oxidation of aniline gave a black powdery deposit on the electrode that was insoluble in water and many organic solvents [5].

The modern era of conducting polymers began at the end of the 1970s when Heeger and MacDiarmid discovered that polyacetylene,  $((CH)_x)$ , synthesized by Shirakawa's method, could undergo a 11 order of magnitude increase of conductivity upon charge-transfer oxidative doping with iodine [6]. Polyacetylene (PAC) is the simplest form of conducting polymer that has the characteristic structure of a conjugated  $\pi$ -system extending over a large number of the chain-linked monomer units. Even though polyacetylene had a very high conductivity, its interactability and instability toward oxygen and water made it infeasible for commercialization [7]. Due to its poor properties, conjugated systems other than PAC with aromatic structures and heteroatomic molecules were investigated (Figure 1.1).

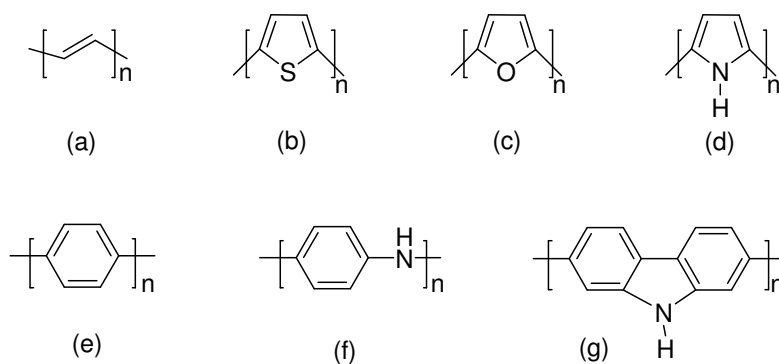


**Figure 1.1** Common conducting polymer structures: (a) polyacetylene, (b) polythiophene, (c) polyfuran, (d) polypyrrole, (e) polyphenylene, (f) polyaniline, (g) polycarbazole

An important step in the development of conjugated poly(heterocycles) occurred in 1979 when it was shown that highly conducting (100 S/cm) and homogeneous free standing films of polypyrrole could be produced by oxidative electropolymerization of pyrrole [8,9]. Although polypyrrole is flexible and stable to water and oxygen, it is interactable and insoluble. Later, the electrochemical polymerization has been extended to other aromatic compounds and heteroatomic compounds including thiophene, furan, aniline, and carbazole.

Due to their higher environmental stability and structural versatility which allow to modulation of their electronic and electrochemical properties by manipulation of the monomer structure, these CPs have rapidly become the subject of considerable interest.

Apart from polyaniline, all of these systems share one common structural, namely a rigid body brought about by the  $sp^2$  carbon based backbone. The utilization of the conjugated construction affords polymer chain possessing extended  $\pi$ -systems, and it is the feature alone that separates CPs from their other polymeric counterparts [10].

Although the initial interest in conjugated polymers was entirely due to their ability to conduct electricity, the current technology developing around these materials is multi-faceted. The focus shifted from simply maximizing electrical conductivity to creating advanced materials with tailored optical, structural, and electrical properties.

Conducting polymers have become of very great scientific and technological importance since 1990 due to their various uses such as components in light-emitting diodes [11].

## **1.2. Band Theory and Conduction Mechanism in Conducting Polymers**

The essential structural characteristic of all conjugated polymers is their quasi-infinite  $\pi$ -system extending over a large number of recurring monomer

units. The simplest possible form is of course the archetype polyacetylene  $(CH)_x$  shown in Figure 1.2. The delocalized  $\pi$ -electron system confers conducting properties to the polymer and gives it the ability to support positive and negative charge carriers with high mobilities along the polymer chain.



**Figure 1.2** Conjugated polymer structure (a) cis-polyacetylene and (b) polythiophene

### 1.2.1. Band Theory

Electronically conducting polymers are extensively conjugated molecules, and it is believed that they possess a spatially delocalized band-like electronic structure. Band theory is used to explain the electronic structure and conduction mechanism of materials. Within this theory, materials are defined as insulators, semiconductors, or metals depending on the relative separation of occupied and unoccupied energy states.

These bands stem from the splitting of interacting molecular orbitals of the constituent monomer units in a manner reminiscent of the band structure of solid-state semiconductors [12,13]. In the solid state, the atomic orbitals of each atom overlap with the same orbitals of the neighboring atoms in all directions to produce molecular orbitals similar to those in small molecules. Polymerization of the monomer to form a polymer causes the highest occupied molecular orbital (HOMO) and the lowest unoccupied molecular orbital (LUMO) to split, forming two separated energy bands called the valence band (VB) and conduction band (CB), respectively (Figure 1.3). The energy difference between the two bands is termed as the band gap ( $E_g$ ).

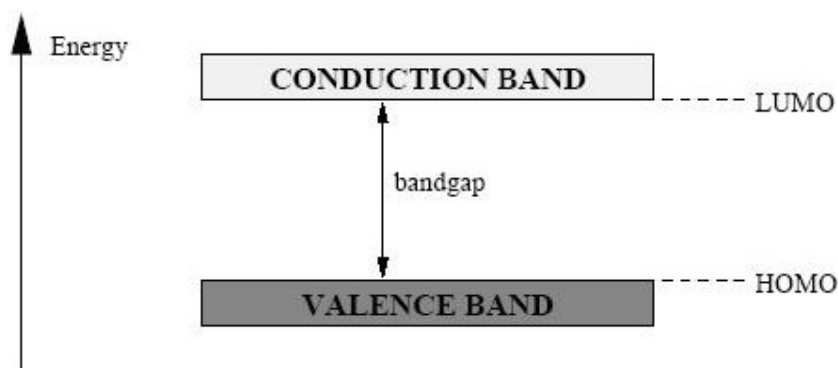


**Figure 1.3** Band structure in an electronically conducting polymer

The band gap can be measured by the absorption band edge in the UV-vis spectrum of a conducting polymer. The absorption band edge is the minimum energy needed to excite an electron to the conduction band from the valence band, which represents the real energy gap between these two bands. However, sometimes the absorption maximum is used and referred as the band gap. Another way to determine the band gap is to measure the oxidation and reduction potentials of the polymer. The energy difference between these two gives the band gap [14].

Figure 1.4 illustrates the generic band structure for a metal, a semiconductor and an insulator. The major difference between these materials lies in the gap between the valence and conduction bands. In metals, there is no energy gap between the valence and conduction bands, and electrons can easily flow through the material. Insulators are characterized by a relatively large energy gap between the two bands which contributes to the low conductivities observed in insulating substances. The behavior of semiconductors is dominated by electrons in states close to the top of the valence band or the bottom of the conduction band. In semiconductors the conduction band is separated from the valence band by an energy gap ranging from 1-4 eV. This

range of energies correlates to the visible spectrum and is associated with electronic transitions [15], hence these materials often display intense color.

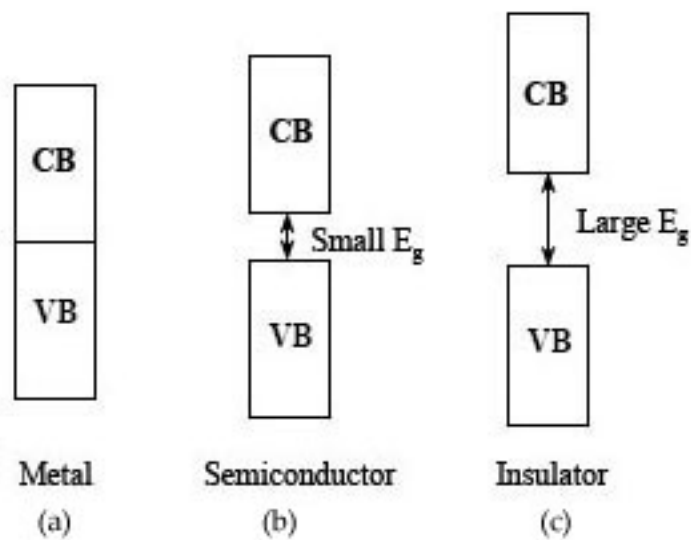


**Figure 1.4** Band structure for (a) a metal (b) a semiconductor and (c) an insulator

The band structure of a conjugated polymer originates from the interaction of the  $\pi$ -orbitals of the repeating units throughout the chain [16]. This is exemplified in Figure 1.5.

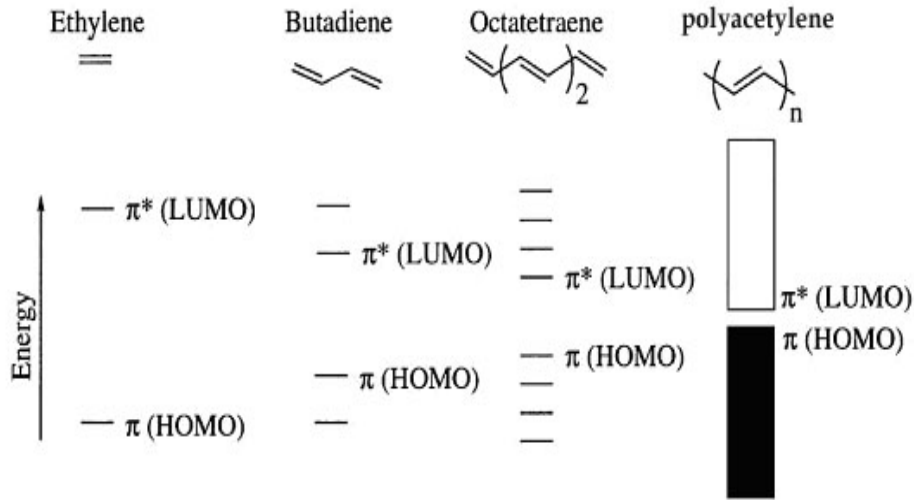


**Figure 1.5** Generation of bands in conjugated polymer systems

As the number of repeating units become sizeable, the electronic levels no longer have discrete energies but rather display a one-dimensional band of allowed energies. Interactions between adjacent and stacked  $\pi$ -electrons of conjugated polymers lead to two and three-dimensional band structure [17].

## 1.2.2. Conduction Mechanism

### 1.2.2.1. Charge Carriers

It is generally agreed that the mechanism of conductivity in the conjugated polymers based on the motion of charged defects within the conjugated framework. The charge carriers, either positive p-type or negative n-type, are the products of oxidizing or reducing the polymer, respectively. The following overview describes these processes in the context of p-type carriers although the concepts are equally applicable to n-type carriers.

Polythiophene (PTh) has a non-degenerate ground state and two mesomeric structures, the aromatic and the quinoidal form [18]. The structural changes that occur for polythiophene upon oxidation are described in Figure 1.6 [19]. When polythiophene chain (Figure 1.6 A) is oxidized (p-doped) and electron is removed from the valence band and a radical cation is formed. The radical cation is partially delocalized over several structure units and called as polaron (Figure 1.6 B). To maintain the electroneutrality, counterions diffuse into the polymer. Further oxidation of the polymer causes polarons (Figure 1.6 C) in the same chain to combine into bipolarons (Figure 1.6 D). When a great many bipolarons are formed (highly p-doped), their energy states overlap at the edges which creates narrow bipolaron bands in the gap. Similar states are formed when the polymer is reduced (n-doped), but the energy levels are below the conduction band [20]. Both polarons and bipolarons are mobile and can move along the polymer chain in an electrical field and hence conduct electrical current.

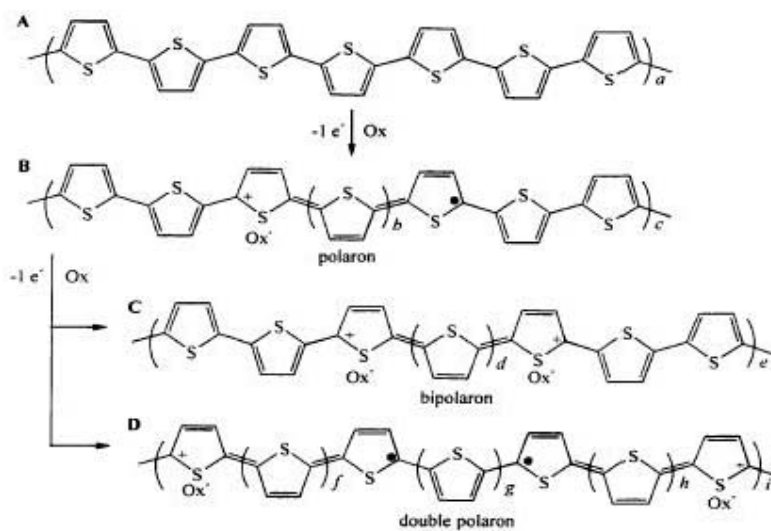


**Figure 1.6** Structural changes in polythiophene upon doping with a suitable oxidant

### 1.2.2.2. Concept of Doping

The electrical conductivity of a conjugated polymer can be increased by several orders of magnitude from insulating or semi-conducting ( $10^{-10}$  to  $10^{-5}$  S.cm<sup>-1</sup>) regime to metallic regime (1 to  $10^4$  S.cm<sup>-1</sup>). The process which enhances the conductivity of a polymer by incorporating a certain “impurity” is known as the “doping”. Doping of conducting polymers has been accomplished by redox processes. This involves the partial addition (reduction) or removal (oxidation) of electrons to or from the  $\pi$ -system of the polymer backbone [21,22]. It should be noted that doping and dedoping are generally reversible which do not change the chemical nature of the original backbone (Figure 1.7).

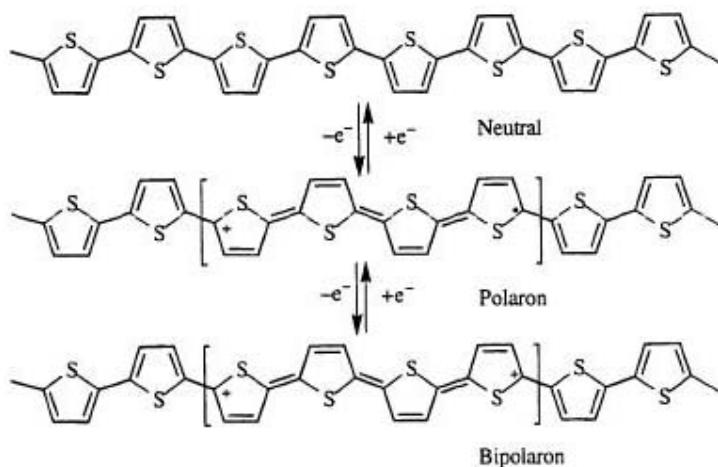
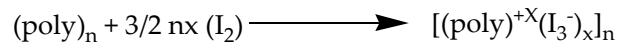


**Figure 1.7** Reversible doping-dedoping process of polythiophene

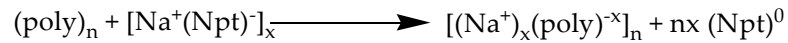
Conducting polymers can be doped either by chemical or electrochemical means. In the chemical pathway, doping is performed by reacting the polymer with suitable oxidizing or reducing agents.

Electrochemical doping is performed by biasing the polymer film in a suitable solution to an appropriate potential [23].

Chemical doping can be performed either by reaction with gaseous species, such as AsF<sub>3</sub>, PF<sub>3</sub>, or I<sub>2</sub>, or in solution by reaction with FeCl<sub>3</sub> in aqueous solution. The chemical reaction describing the oxidative p-doping of a polymer with I<sub>2</sub> can be written as



It is usual for n-type doping of a polymer to be performed with sodium naphthalide (Na<sup>+</sup>Npt<sup>-</sup>) in tetrahydrofuran solution



where poly is a π-conjugated polymer; n is the number of polymers; and x is amount of charge transfer from a polymer chain to counter ions [24,25].

By adjusting the doping level, a conductivity anywhere between that of the non-doped (insulation or semiconducting) and that of the fully doped (highly conducting) form of the polymer can be easily obtained (Figure 1.8) [26].

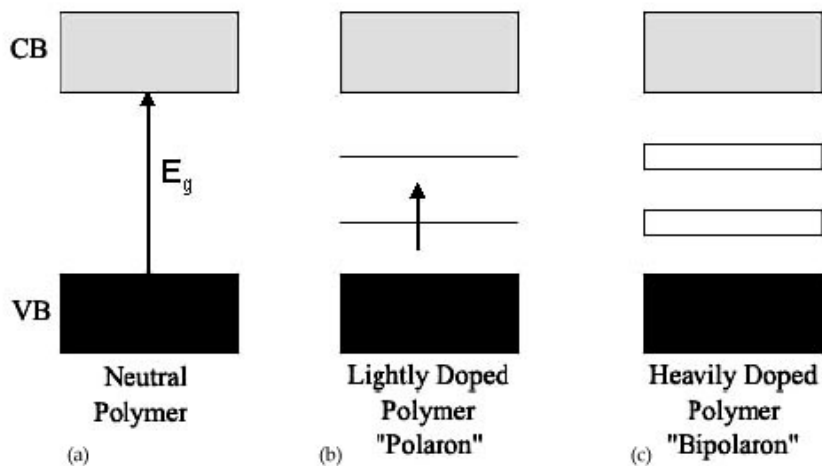


**Figure 1.8** Band model of (a) non-doped, (b) slightly doped, and (c) heavily doped conducting polymers

Electrochemical doping is most useful to give way to control doping process. In electrochemical doping, the electrode gives (accepts) electrons to (from) the conjugated polymers in reduction (oxidation) process, at the same time counterions in the electrolyte diffuse into (or out) the polymer chains for charge compensation. The relative positions of the Fermi level of the substrate ( $E_{F,m}$ ) with respect to either the valence band ( $E_{VB,p}$ ) or the conduction band ( $E_{CB,p}$ ) of the polymer determines whether electrons are extracted (p-doping) or inserted (n-doping).

If the Fermi level of the substrate is below the valence band of the polymer, a flow of electrons from the polymer to the substrate will occur (Figure 1.9 (a)). This is termed p-doping. Likewise, if the Fermi level of the substrate is above the conduction band of the conducting polymer, then electrons flow into the film (Figure 1.9 (b)). This is termed as n-doping.

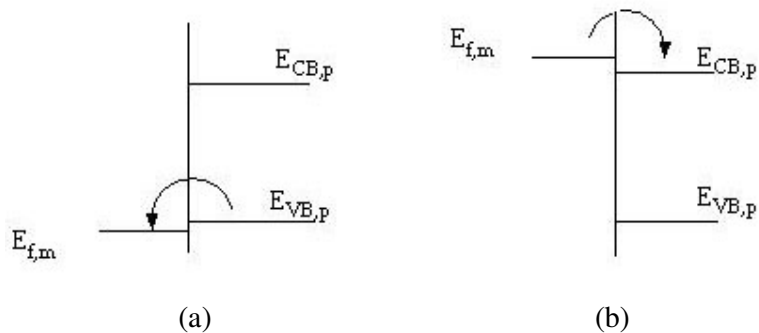


**Figure 1.9** Schematic illustration of doping (a) p-doping and (b) n-doping of conducting polymers [27]

The homogeneous doping level of the system is determined by the cell voltage at electrochemical equilibrium which is the potential difference between the working and the counter electrodes. Thus, the doping level is precisely defined at electrochemical equilibrium [28].

Electrochemical doping is illustrated by the following examples:

For p-type:



For n-type:



where sol'n is solution and elec'd is electrode.

Figure 1.10 illustrates the range of conductivities in CPs and their comparison with other materials. The magnitude of this change varies with doping levels, which can be controlled by the applied potential in the case of electrochemical doping [11].

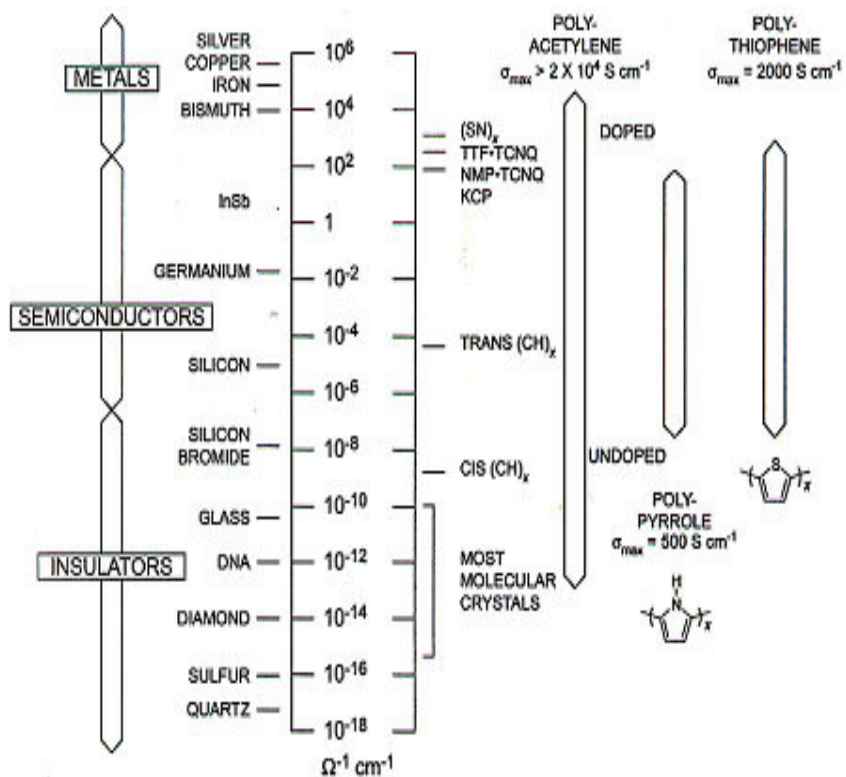


**Figure 1.10** Conductivities of some metals, semiconductors and insulators

### 1.2.2.3. Hopping

A great deal of effort has been devoted to the characterization and understanding of electrical transport in conducting polymers. A main factor limiting the conductivity is the carrier mobility, not the carrier concentration.

The doping process produces a generous supply of potential carriers, but to contribute to conductivity they must be mobile [29].

The movement of electrical charges along the polymer chain, called intra-chain movement (Figure 1.11 A), and also jumping from one chain to another, called inter-chain movement (Figure 1.11 B). The intra-chain movement depends on the effective conjugation of the polymer, while the inter-chain jumping is determined by the stacking of the polymer molecules. Conductivity is not only a result of charge transfer along the chain, but it is also due to electron hopping between conjugated segments of the same chain (Figure 1.11 C).

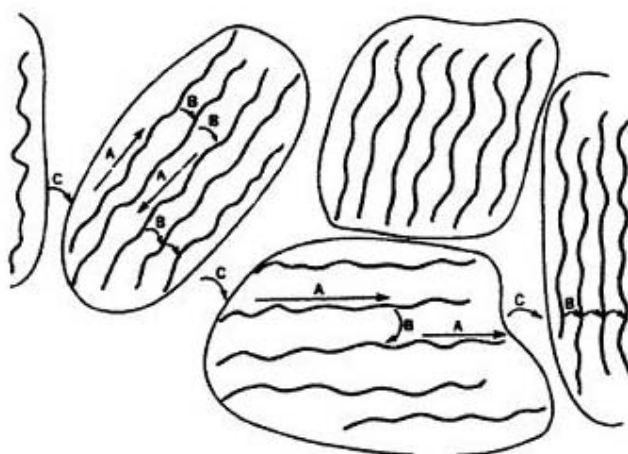


**Figure 1.11** Charge carrier transport in a conducting polymer

Therefore, the overall mobility of charges is related to intra-chain, inter-chain, and inter-particle mobilities. These three elements comprise a complicated resistive network which determines the effective mobility of the carriers. Thus, the mobility,  $\mu$ , and therefore, the conductivity are determined on both a microscopic (intra- and interchain) and a macroscopic (interparticle) level.

Various hopping models have been proposed to describe conduction mechanism. In the Mott model of variable range hopping, conductivity is given by

$$\sigma = \sigma_0 \exp [-(T_0/T)]^\gamma$$

where  $\sigma_0$  and  $T_0$  are constants and  $\gamma$  is a number,  $1/4 \leq \gamma \leq 1/2$ , related to the dimensionality,  $d$ , of the hopping process via [31]

$$\gamma = 1/1+d$$

In the polymer systems considered here, dimensionality refers to the type of transport available to the charge carriers. For most polymeric materials the electronic conduction is 3-D, therefore, a linear  $\log \sigma$  vs.  $T^{-1/4}$  dependence has been widely used as an evidence for transport via variable range hopping [32,33].

### **1.3. Synthesis of Conducting Polymers**

While there is no single method for synthesizing conducting polymers, the incorporation of extended  $\pi$ -electron conjugation is of foremost importance. Conductive polymers may be synthesized using standard methods of polymerization including electrochemical, chemical polymerization as well as specific routes which include Grignard reaction, ring-opening metathesis and transition metal-catalyzed polymerization [34]. Polymers obtained by a chemical procedure are in their insulating form and can be chemically or electrochemically doped to their conducting form. In contrast, polymers generated electrochemically are in their oxidized, conducting state. The thickness and morphology of the polymer film can be controlled during the electrolysis process [35].

### 1.3.1. Chemical Polymerization

The synthesis of pristine polymers which exhibit metallic character upon doping can be achieved by two common chemical methods: (I) oxidation of monomers in the presence of excess ferric chloride ( $\text{FeCl}_3$ ) or other transition metal chloride; (II) catalytic Grignard coupling of 2,5-dihalothiophenes especially by nickel catalysts [36].

In most cases, addition polymerization involves the repeated addition of an unsaturated monomer to an active center such as a radical or an ion. The oxidizing force is supplied by a chemical oxidant in the solution. The most widely employed oxidizing agent has been  $\text{FeCl}_3$ . For the synthesis of polypyrrole, one-electron oxidants such as  $\text{FeCl}_3$ , an [oxidant/pyrrole] molar ratio ca. 2.3 is usually employed. Two electrons are required for the oxidation of each pyrrole unit, with the remaining 0.3 electrons being used for ca. 30% oxidative doping of the neutral PPy into its conducting form where the polymer carries one positive charge on every three pyrrole units on the average (Figure 1.12) [37].

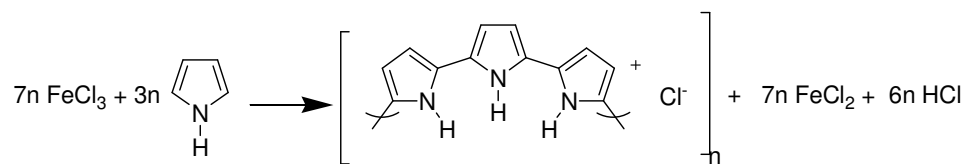


**Figure 1.12** Oxidative chemical polymerization of pyrrole in the presence of iron (III) chloride

The controlled chemical synthesis of polythiophene is performed by metal-catalyzed coupling of 2,5-dibromothiophene (Figure 1.13). The dibromothiophene substrate is reacted with Mg in THF, replacing either 2- or 5- bromo substituent with  $-\text{MgBr}$ . Self coupling is then achieved with metal

complex catalyst such as Ni(bipy)Cl<sub>2</sub>, the condensation reactions eventually lead to polythiophene without undesirable 2,3' and 2,4'-couplings [38].

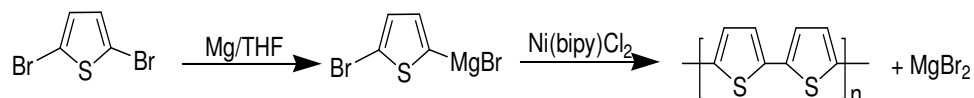


**Figure 1.13** Chemical polymerization of polythiophene in the presence of metal-catalyze

Although chemical methods for the synthesis of conducting polymers have the advantages of low cost, speed, and freedom from the restrictions of electrodes, there are many problems that are inherent to chemical polymerizations. Because the polymer is formed in its oxidized form, which is believed to be more rigid than the neutral form, the oxidized polymer chains can precipitate from the polymerization medium limiting degree of polymerization. Overoxidation and decomposition can also occur in these polymerizations as a result of the strong oxidizing agents used [39].

### 1.3.2. Electrochemical Polymerization

Electrochemical polymerization is often used to prepare redox active polymer films on electrode surfaces. Electrochemical syntheses of poly(heterocycles) have been carried out by an anodic or a cathodic route (Figure 1.14).

The major drawback of the electroreduction method is that the polymer is produced in its insulating form which leads to a passivation of the electrode and limits attainable film thickness [40].

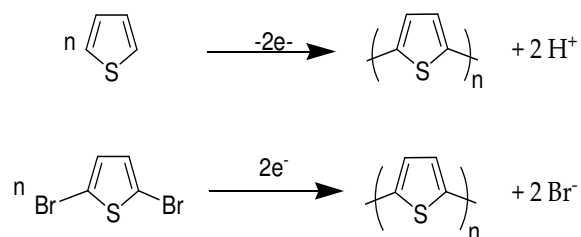


**Figure 1.14** Electrochemical synthetic routes to polythiophene

The oxidative electrochemically prepared polymers usually show improved properties compared to those prepared by the chemical and the electroreduction method. Compared with other chemical and electrochemical methods, the advantages of oxidative electropolymerization are the followings [41,42]:

- (i) A highly electrochemically active and conductive polymer film can be easily produced on an electrode, which can be directly used as an electrode in a battery or a sensor.
- (ii) Film thickness, morphology and conductivity can be easily controlled by the applied potential, polymerization time, and the electrochemical potential scan rate.
- (iii) They provide an in situ way to investigate the polymerization process and the properties of the resulting conducting polymer by electrochemical or spectroscopic techniques.

The electropolymerization conditions have been found to affect the structure and properties of the resulting polymers to a large extent.

### 1.3.2.1. Mechanism of Electrochemical Polymerization

Figure 1.15 represents the mechanism proposed for the electropolymerization of heterocycles by anodic coupling. The first electrochemical step (E) consists of the oxidation of the monomer to its radical cation. Since the electron-transfer reaction is much faster than the diffusion of the monomer from the bulk solution, it follows that a high concentration of radicals is continuously maintained near the electrode surface. The second step is controversy step because coupling may proceed via two different routes. The coupling proceeds either by the combination of two radical cations or addition of radical cation to heterocyclic monomer. In the radical-radical coupling, the second step involves the coupling of two radicals to produce dihydro dimer dication which leads to a dimer after loss of two protons and rearomatization. This rearomatization constitutes the driving force of the chemical step (C). Due to the applied potential, the dimer, which is more easily oxidized than the monomer, occurs in its radical form and undergoes a further coupling with a monomeric radical.

In a radical–monomer coupling mechanism, the radical cation reacts with the monomer to yield a neutral dimer by the loss of another electron and two protons. The oxidized dimer radical cation again attacks a monomer to form a trimer and the propagation proceeds to form polymer. Electropolymerization proceeds then through successive electrochemical and chemical steps according to a general  $E(CE)_n$  scheme, until the oligomer becomes insoluble in the electrolytic medium and precipitates onto the electrode surface [43,44].

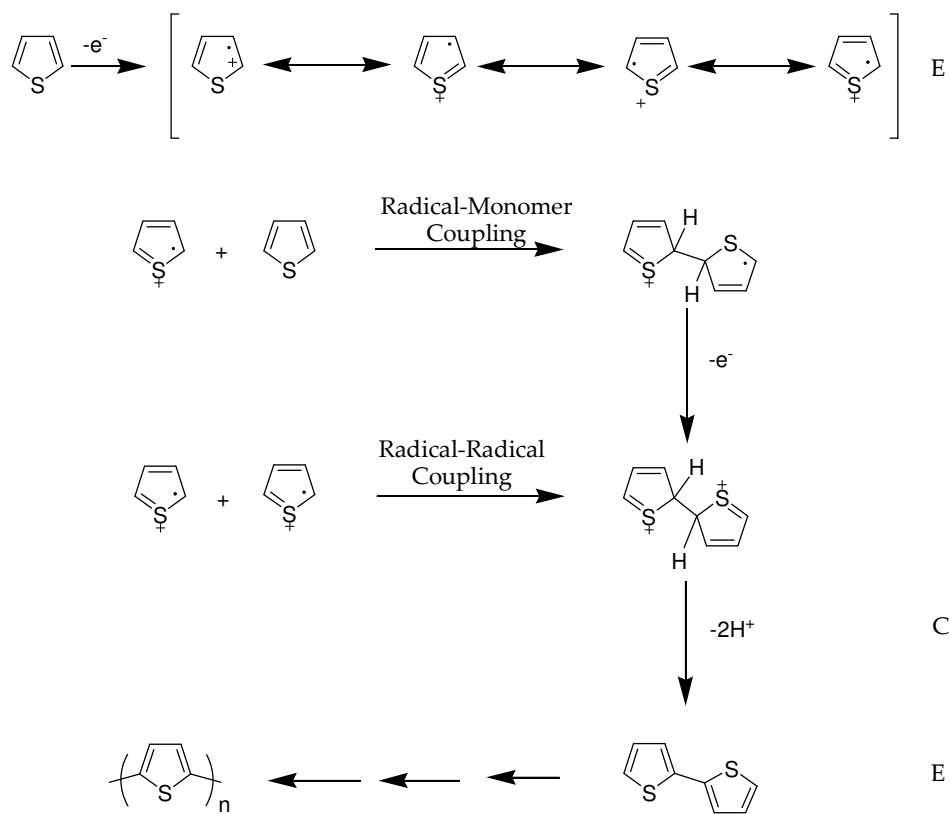


**Figure 1.15** Proposed mechanisms for the electropolymerization of thiophene

### 1.3.2.2. Effects of Electrolytic Conditions

The electrical properties and the morphology of the film are affected by the type of solvent used, the nature of electrolyte employed, the amount of current or potential applied to the cell, and the temperature maintained during the course of the electrosynthesis.

The solvent must possess two attributes in order to be classified as an adequate medium for polymerization. It must have high dielectric constant in order to allow for ionic conductivity and be stable over a broad potential range

such that solvent redox processes do not interfere with electrochemical processes occurring during polymerization. Since oxidative electrochemical polymerization involves the formation of radical cations, the nucleophilicity of the solvent should be kept low. Polar aprotic solvents like acetonitrile or propylene carbonate have very large potential windows, and high relative permittivities, which allow a good dissociation of the electrolyte and hence a good ionic conductivity [45,46].

Supporting electrolyte is used to provide electrical conductivity. The electrolyte dopes the polymer by allowing one of its ions to couple with a monomer unit. The electrolyte chosen during the polymerization has been shown to significantly affect the morphology and electrochemical properties of the conducting polymer [47]. The nature of the anion used during the synthesis step plays a determining role on the structure of the polymer. The nature of the cation, on the other hand, affects essentially the behavior of the polymer films during the charge-discharge processes. Conducting polymers are generally electrogenerated in the presence of lithium or tetraalkylammonium salts of either  $\text{ClO}_4^-$  or  $\text{BF}_4^-$  [48].

The monomer concentration is generally high (0.1 M or more) to avoid competitive reactions of the radical cations or of the oxidized polymer with nucleophiles in the medium. The probability of the occurrence of these reactions depends on the oxidation potential of monomer. While the oxidation potential of the monomer decreases, the occurrence of the competition reaction also decreases. Therefore, millimolar concentrations may be used to perform efficient polymerization [49].

The polymers are generally deposited on inert substrate such as platinum and gold or optically transparent electrodes such as indium-tin-oxide (ITO) coated glass. The most conductive polymers have been obtained on bulk platinum, presumably because thiophene adsorbs more efficiently on platinum and also presents a larger number of potentially active sites leading to a high density of nucleation sites and to more compact materials.

### **1.3.2.3. Monomer Structure and Substituent Effects in Electropolymerization**

Convenient and reproducible syntheses are required before materials can be developed for a particular application. In recent times an extensive worldwide research effort has been specifically directed towards synthetic aspects, since the structure and reactivity of the monomer will greatly affect the properties of the resulting polymer.

Although considerable success has been obtained using conducting polymers containing  $\pi$ -conjugated systems, many of these polymers have problems with processability and mechanical properties. Due to electron transfer and coupling, interchain interactions in  $\pi$ -conjugated polymers are relatively strong. These polymers are often insoluble in common organic solvents and infusible. It is usually difficult to characterize their structure, understand electronic interactions and process them. This greatly limits their practical applications [50].

Electron-rich heterocycles such as Th and Py are the most common monomers for electropolymerization due to their availability and relative ease of polymerization. Since PTh have shown higher chemical and electrochemical stability in air and moisture in both their doped and undoped states than others such as polypyrrole, thiophene-based polymers have received significant attention.

Substitution is a very powerful tool for the design of thiophene-based polymers for different applications. The character and position of the side chain will influence properties like solubility, band gap, ionic conductivity, morphology and miscibility with other substances [51].

Electronic effects arising from electron-withdrawing and electron-donating substituents drastically affect the electron density of the thiophene ring. Thiophenes substituted with electron-withdrawing groups such as cyano, aldehydes and nitro groups have oxidation potentials that are higher than

thiophene, and they do not electropolymerize. In the case of electron-donating groups, the oxidation potential decreases due to the stabilization of the radical cation formed upon oxidation.

Substituents not only affect the oxidation potential of the monomers and polymers, but also the band gap and optical absorption of these systems. Electron-donating groups lower the band gap by raising the valence band or HOMO level. This is illustrated by comparing the band gaps of polythiophene (2.0 eV) and poly(3,4-ethylenedioxythiophene) (PEDOT) (1.6 eV) [52].

The addition of relatively long, flexible, hydrocarbon chains to the thiophene ring has increased solubility and processibility of this conjugated polyheterocycles without significantly changing the  $\pi$ -electronic structure. The electronic absorption spectra of the poly(3-alkylthiophenes) (P3AThs) indicated that the band gap is about 2eV, a value that is typical for the entire P3AThs (Figure 1.16). The color variations have been ascribed to changes in the effective conjugation length of the polymer chain [53].

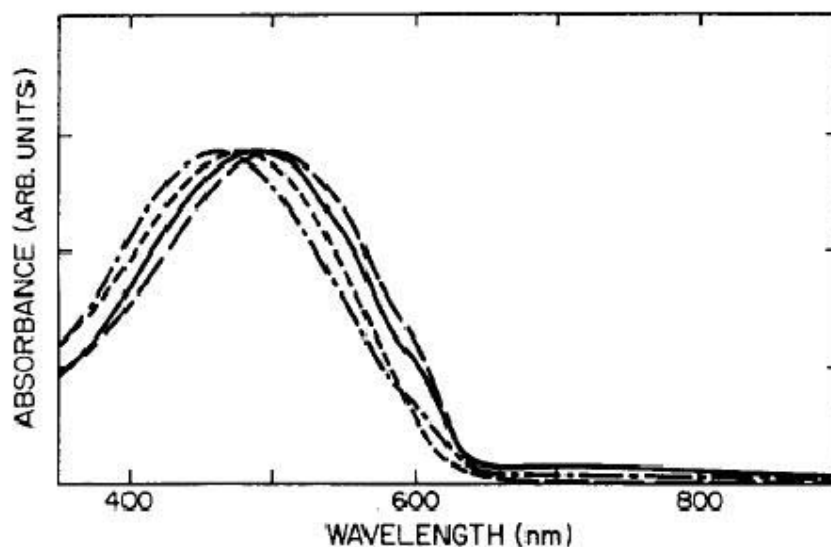


**Figure 1.16** Absorption spectra of PTh and a few alkyl derivatives of 3-substituted PThs: (---) PTh; (---) P3MTh; (— . — .) P3BTh; (— —) P3HTh

Basically, substituent groups on the 3- and/or 4-positions of the thiophene ring minimizes the occurrence of mislinkages such as  $\alpha$ ,  $\beta$  coupling or  $\beta$ ,  $\beta$  coupling during polymer synthesis (Figure 1.17). The occurrence of a  $\alpha$ - $\beta$  linkage in a given chain modifies its electronic distribution and could promote the formation of branching in energetically favorable sites. Furthermore, the presence of these linkage defects twists in adjacent chains, and thus modifies their electronic distribution promoting the propagation of more defects in the resulting materials. This is consistent with the considerable increase in the content of disorder as well as the decrease in conductivity as the polymerization proceeds. Fewer  $\alpha$ - $\beta$  linkage defects in the final structures lead to more effective conjugation, which is an essential feature to produce more conductive polymer [54].

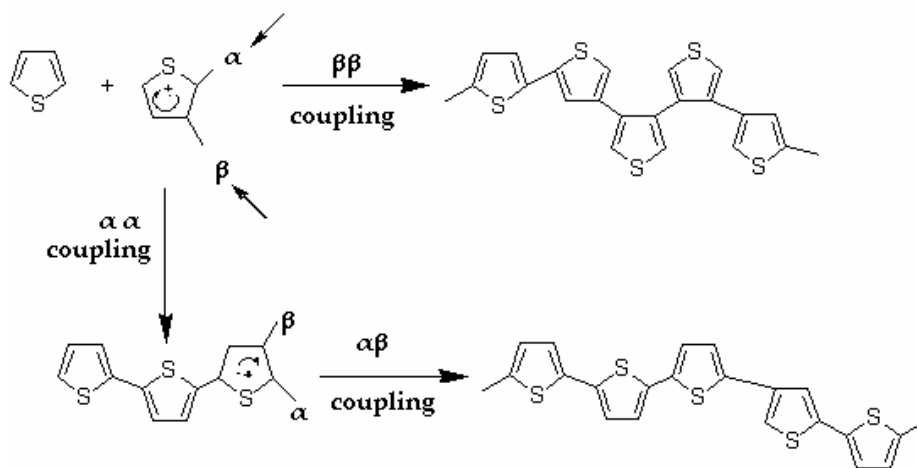


**Figure 1.17** Competitive reaction pathways in unsubstituted polythiophene

In general, disubstitution at the 3 and 4 positions, which eliminates the possibility of  $\beta$  coupling and reduces the likelihood of cross-linking, leads to severe steric interactions and reduces the extent of conjugation. 3,4-Dialkyl

substitution results in severe steric hindrance, decreasing conjugation. Alkoxy substituents were found to lower conductivity as a consequence of repulsive interaction between adjacent side chains. Monomers containing 3,4-dialkoxy substituents are also poorly reactive to oxidative polymerization because of stabilization caused by conjugation with the thiophene [55]. These are overcome by fusing the ring onto the heterocycle, effectively pinning the substituents back from the main chain.

By introducing an alkyldioxy group to thiophene at the 3- and 4-positions, the electron-donating benefits are maintained, and the steric effects are eliminated. Alkylenedioxy substituents are also too strained for a high level of conjugation with thiophene ring allowing them to polymerize easily. Table 1.1 summarizes the effects of substitution on electrochromic properties of the parent monomer thiophene.

**Table 1.1** Electrochromic properties of thiophene derivatives

Monomer	Polymer $\lambda_{\text{max}}$ and color		Eg (eV)
	Oxidized state	Reduced state	
Thiophene	730 nm (blue)	470 nm (red)	1.9 eV
3-Hexylthiophene	800 nm (deep blue)	435 nm (red)	1.7 eV
EDOT	1100 nm (sky blue)	610 nm (red)	1.6 eV

The electrochemical synthesis of conducting polymers from multi-ring aromatic monomers with electron-rich terminal heterocycles has attracted considerable attention as they have significantly lower oxidation potentials than the corresponding parent heterocycle due to the extended conjugation of the multi-ring system. The presence of electron-rich heterocycles (e.g., pyrrole, thiophene, 3,4-ethylenedioxythiophene) as terminal electropolymerizable moieties on multi-ring conjugated monomers leads to stabilization of the cation

radical intermediates allowing to proceed at low potentials and with minimum side reactions. These include  $\beta$ -coupling, crosslinking, and overoxidation of the resultant polymer leading to polymer degradation and defect-containing materials [56,57].

#### **1.4. Conducting Copolymers**

Syntheses of conducting random, block and graft copolymers are shown to be effective ways to compensate the certain deficiencies of conducting polymers like poor mechanical, physical and chemical properties. Two monomers could be polymerized to synthesize the conducting copolymer with different properties than their corresponding homopolymers [58,59].

Electrochemical polymerization of the conducting component on an electrode previously coated with the insulating polymer is one of the most widely used methods for that purpose. A second type of copolymer involves two electroactive monomers. Today, the synthesis of copolymer is mainly performed with 3,4-ethylenedioxythiophene (EDOT) that is superior to its parent polythiophene in many categories crucial to organic electrochromic materials such as rapid switching and lower oxidation potentials [60]. In this way, the resultant copolymer could indicate better electrochemical and optical properties than its homopolymers.

#### **1.5. Characterization of Conducting Polymers**

Conventional techniques for polymer characterization cannot be applied to all conductive polymers, since the highly conjugated backbone causes insolubility in common solvents. Therefore, the following are mostly used to characterize conductive polymers. Primary characterization of CPs is done by cyclic voltammetry that shows the potentials at which oxidation or reduction process occurs, the degree of reversibility of the electrode reaction

[61]. FTIR spectroscopy has always found wide applications in the characterization of polymeric materials. The utility of FTIR spectroscopy arises from its ability: i) to differentiate between functional groups, ii) to identify specific polymer systems, iii) its quantitative character with calibration, and iv) its speed and low cost [62]. Structural information can be provided by X-ray photoelectron spectroscopy (XPS), transmission electron microscopy (cross-section of surface)(TEM) and atomic force microscopy(surface roughness). Morphology of CPs film has been described by scanning electron microscopy [37].

## **1.6. Applications of Conducting Polymers**

With the advantage of high electronic conductivity combined with flexible and plasticity, the applications of conducting polymers have been the focus of intensive study in recent years. Applications of conducting polymers can be divided into three main classes. The first use of conjugated polymers is in their neutral form, and takes advantage of their semi-conducting and luminescent properties. One of the examples of applications that use conjugated polymers as semiconducting materials is field effect transistors [63]. The second category involves using the polymer in its doped or conducting form for EMI shielding and as electrode materials for capacitors. The third category uses the ability of the polymer to switch reversibility between its conducting and reduced forms. Upon switching between the two states, the polymer undergoes color, conductivity and volume changes. Applications that use these properties include battery electrodes, mechanical actuators, sensors, drug delivery and electrochromics [64,66].

## 1.7. Chromism

Chromic behavior is another characteristic of CPs. Thermochromism, solvatochromism, piezochromism, ionochromism and electrochromism for CPs have been reported. These different chromic behaviors originate from conformational modification and the energy change in  $\pi$ - $\pi^*$  transition band gap induced by the corresponding environmental changes such as temperature, solvent power, pressure, ion strength, and applied potential, respectively [67].

### 1.7.1. Electrochromism

An electrochromic material is the one where color change is brought about by an electrochemical redox reaction. Color changes are commonly between a transparent (bleached) state, where the chromophore only absorbs in the UV region, and a colored state or between two colored states. When more than two redox states are electrochemically accessible in a given electrolyte solutions, the electrochromic material may exhibit several colors and be termed as polyelectrochromic [68].

Many materials possess this characteristic, with the most common ones being metal oxides, organic dyes, and more recently, conducting polymers. CPs are suitable candidates due to their processability, stability, color tenability, electrical conductivity, and the possibility to be fabricated into large, flexible flat sheets [69].

As mentioned in Section 1.2.2.2., the doping process of a conducting polymer involves a structural modification of the backbone from a totally aromatic neutral form to a doped state with quinoidal partitions. This change in structure is accompanied by a change in the electronic transitions from a higher energy to a lower energy. Since these transitions for the most part lie in the visible region, a color change is induced, with a transformation from a more optical transparent to a more optically opaque material or vice versa [70].

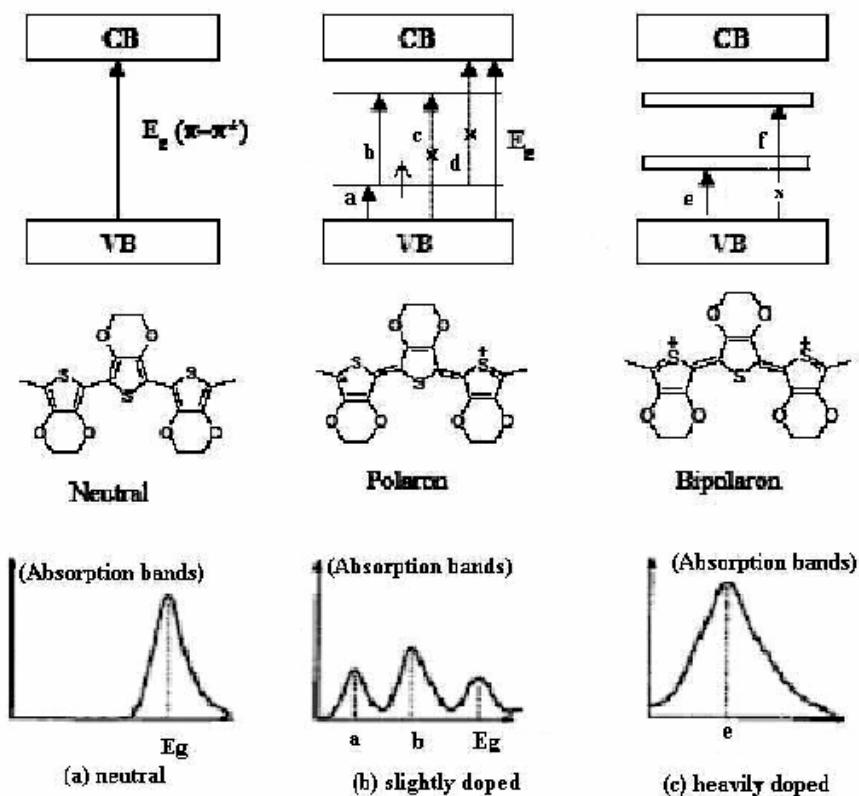


**Figure 1.18** Polaron and bipolaron in non-degenerate ground state polymers: band diagrams for neutral (a), positive polaron (b) and positive bipolaron (c)

Figure 1.18 shows the general features of the doping-induced electronic structure and the corresponding optical-absorption bands of nondegenerate ground-state polymers. In the neutral state the polymer exhibits one transition from the valence to the conduction band ( $\pi$ - $\pi^*$ ). The energy difference between these two levels is the band gap ( $E_g$ ), and it is the measure as the onset of the  $\pi$ - $\pi^*$  absorption in the neutral state of the polymer (Figure 1.18 (a)). The polaron is the expected state when the system is lightly doped. This result in the state is higher than the valence band. There is also a lowering of the corresponding antibonding level in the conduction band, and two intragap states are introduced. Although four new transitions are expected, two

low energy transitions occur, since the oscillator strength of transitions a and b are much greater than the transitions c or d (Figure 1.18 (b)). Therefore, the signature of a polaron is the two low energy transitions [71]. Further oxidation of polymer creates the bipolaron state. Since the bipolaron levels are unoccupied, only transitions from the valence band can occur. Transition e is much stronger than f, so one low energy transition is expected as the signature for a bipolaron.

### 1.7.2. Types of Electrochromic Materials

A large variety of materials are known to display electrochromism. They are divided in four general classes: a) transition-metal oxides (e.g.  $\text{WO}_3$ ,  $\text{IrO}_2$  etc.), b) conductive polymers, c) organic and d) intercalated materials. They are also classified as cathodic and anodic electrochromic materials, depending on the coloration mechanism [72].

Crystalline  $\text{WO}_3$  is one of the most studied electrochromic materials not only as a result of its transparent/ intense blue electrochromism ,but, it also has some specific switching properties in the infrared region, of relevance to 'smart windows' technology. Although complementary electrochromic windows based on cathodically coloring  $\text{WO}_3$  and anodically coloring  $\text{IrO}_2$ , have been fabricated, their development is still limited. Due to their high cost for fabrication and short term stability, extended works have been carried out on conductive polymers [73].

Conductive polymers are classified into three groups in terms of their electronically accessible optical states. The first type includes material with at least one colored and one bleached state. These materials are especially useful for absorption/transmission type device application such as smart windows. A second class of materials consists of electrochromes with two distinctive colored states. Poly(3-methylthiophene) is a good example of this type, where the thin films of this polymer switch from red to deep blue upon oxidation. A

third class includes the materials which have two color states depending on the redox state of the material. In this area, conjugated polymers are used due to their versatility for making blends, laminates, and copolymers [74].

The nature of both the color and optical density are dependent on the Eg. High band gap polymers are most opaque in the oxidized form and are defined as being anodically coloring, whereas low band gap polymers are optically dense in the reduced form and are defined as being cathodically coloring [75].

### **1.7.3. Spectroelectrochemistry**

In order to probe the electronic structure of the polymers, and to examine the optical structure of the polymers, and to investigate the optical changes that occur during redox switching which are important for electrochromic applications, optoelectrochemical analyses were carried out [76]. It provides information about the material's band gap and interband states created upon doping as well as gives some insight into a polymer color through the location of the absorption maxima and the ratio of peak intensities if the material shows fine structure on the main  $\pi$ - $\pi^*$  peak.

### **1.8. Electrochromic Devices (ECD)**

The considerable spectral changes in the visible region associated to the doping/dedoping process of conducting polymers have led to several proposals for electrooptical systems such as electrochromic devices [41].

An electrochromic device is essentially a rechargeable battery in which the electrochromic electrodes are separated by a suitable solid or liquid electrolyte from a charge balancing counter electrode, and the color changes occur by charging and discharging the electrochemical cell with applied

potential of a few volts [77]. The second electrode in some systems may also be electrochromic and in any case must undergo electron transfer in the reverse sense to that of the first electrode (Figure 1.19) [78].

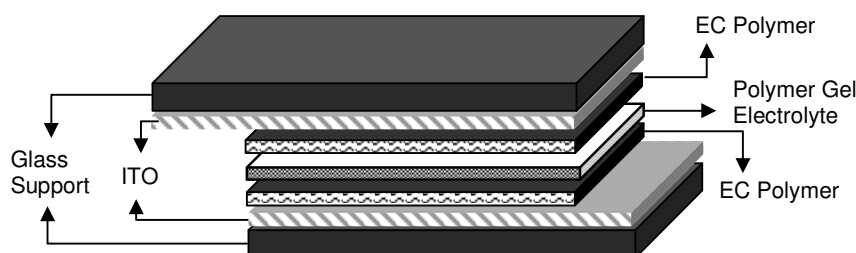


**Figure 1.19** Schematic illustrations of dual type electrochromic device

The arrangement of these layers depends on the operation mode, which can be reflective or transmissive. The reflective mode is used to display or decrease the reflected light, for example, in a car rear-view mirror. In these devices, one of the electrical contacts should be covered with a reflective layer as a mirror [80]. Transmissive mode operation is very similar, but all layers must become fully transparent when desired. For this reason, optically transparent electrodes must be used in the two electrical contacts. The schematic representations of the two operation modes are shown in Figure 1.20.

In order to be useful for applications, electrochromic devices must exhibit long-term stability, rapid redox switching, and large changes in transmittance between states (large T % values) [81].

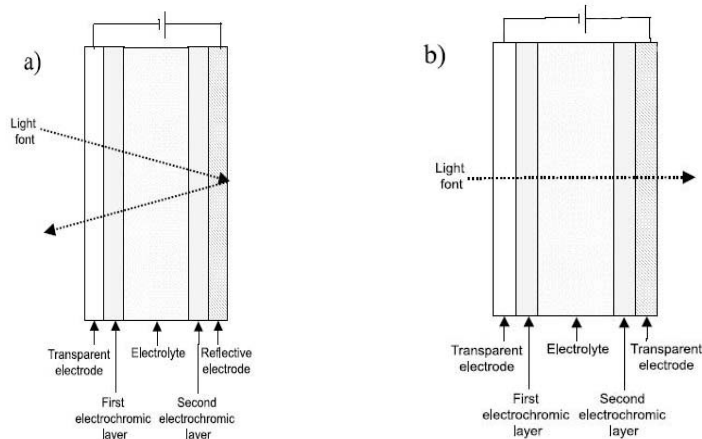


**Figure 1.20** Schematic representations of dual type (a) reflective and (b) transmissive type electrochromic device configurations [79]

## 1.9. Characteristics of Electrochromic Device

To gain a deeper understanding of the electrochromic processes in ECDs, multiple characterization methods have been developed. As discussed in the previous section, spectroelectrochemistry has been commonly used to study the electrochromic processes in conjugated polymers. However, spectroelectrochemistry does not allow one to precisely define contrast ratios or switching speeds. Thus, other methods such as switching, stability, and open circuit memory experiments have been developed in addition to spectroelectrochemistry.

### 1.9.1. Electrochromic Contrast and Switching Speed

One of the important parameters of evaluating an electrochromic material is its electrochromic contrast. Electrochromic switching studies are carried out to monitor absorbance changes with time during repeated potential

stepping between reduced and oxidized states to obtain an insight into changes in the optical contrast. It is often reported as a percent transmittance change ( $\Delta T \%$ ) at specified wavelength where the electrochromic material has the highest optical contrast [82].

The time required to switch between bleached and colored state is reported as the switching time. Morphology of the film, the ionic conductivity of the electrolyte, and accessibility of the ions to the electroactive sites are the factors that affect the switching speed of electrochromic materials.

### **1.9.2. Open Circuit Memory and Stability**

The color persistence in the ECDs is a significant character since it is directly related to aspects involved in its utilization and energy consumption during application. This feature is defined as the optical memory of an electrochromic device. This is the time during which the material keeps its color without an applied potential.

The stability of the polymer for long term switching between oxidized and neutral states is important for practical applications. Electrochromic stability is associated with electrochemical stability since the degradation of the active redox couple results in the loss of electrochromic contrast and hence the performance of the ECDs. Common degradation paths include irreversible oxidation or reduction at extreme potentials, side reaction due to the presence of water or oxygen in the cell [82].

### **1.9.3. Colorimetry**

In-situ colorimetry analysis is used as a means of precisely defining color and contrast ratio in electrochromic polymers. Colorimetry provides a more precise way to define color than spectrophotometry. Rather than measuring absorption bands, colorimetry measures the human eye's sensitivity

to light across the visible region and gives a set of color coordinates to describe color such as the CIE 1931 Lab color space (Figure 1.21).

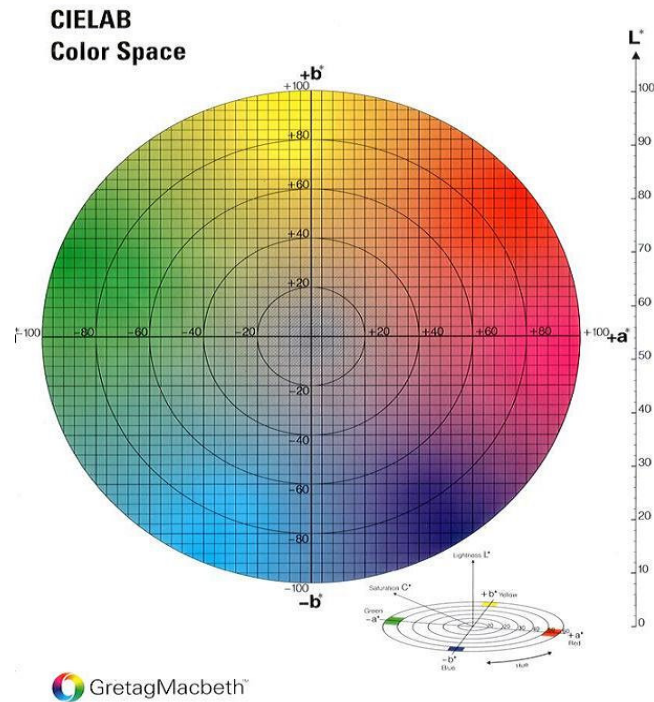


**Figure 1.21** CIE LAB color space

In this color coordinate there are three values in relation to color. A coordinate of color,  $a$ ; defines its hue (dominant wavelength), which is the wavelength where maximum contrast occurs,  $b$ ; coordinate of color is its saturation (purity), which is the color's intensity, and  $L$  corresponds to brightness (luminance) [83,84].

### **1.10. Aims of the Work**

Aims of the work are *i)* to synthesize thiophene functionalized monomer namely as 1-phenyl-2,5-di(2-thienyl)-1*H*-pyrrole (PTP). *ii)* Electrochemically polymerize and copolymerize it with a well known comonomer (EDOT) in thin film forms. *iii)* Examine the electrochromic properties of the homopolymer and copolymer. *iv)* Construct electrochromic devices with PEDOT and finally evaluate the electrochromic performances of these devices.

## CHAPTER II

### EXPERIMENTAL

#### 2.1. Materials

$\text{AlCl}_3$  (Aldrich), succinyl chloride (Aldrich), toluene (Sigma), aniline (Aldrich), *p*-toluenesulfonic acid (PTSA) (Aldrich), iron(III) chloride (Aldrich), NaOH (Merck), tetrabutylammonium tetrafluoroborate (TBAFB) (Aldrich),  $\text{LiClO}_4$  (Aldrich),  $\text{NaClO}_4$  (Aldrich), propylene carbonate (PC) (Aldrich) and poly(methylmethacrylate) (PMMA) (Aldrich) were used as received. Thiophene (Aldrich) was distilled before use. Dichloromethane (DCM) (Merck), nitromethane (Aldrich), methanol (Merck), and 3,4-ethylenedioxythiophene (EDOT) (Aldrich) were used without further purification. Acetonitrile (ACN) (Merck) was dried before use.

#### 2.2. Equipment

The cyclic voltammograms were recorded using VoltaLab PST050 and Solartron 1285 Potentiostats. Measurements were performed at room temperature under nitrogen atmosphere. A Varian Cary 5000 UV-Vis spectrophotometer was used to perform the spectroelectrochemical studies of homopolymer and copolymer and the characterization of the electrochromic

devices. Colorimetry measurements were done via a Conica Minolta CS-100 spectrophotometer.

A Bruker-Instrument-NMR Spectrometer (DPX-400) was used to record  $^1\text{H}$  and  $^{13}\text{C}$  NMR spectra in  $\text{CDCl}_3$ . Chemical shifts were given in ppm relative to tetramethylsilane as the internal standard.

The FTIR spectra were recorded on a VARIAN 1000 FTIR spectrometer. The surface morphology of the homopolymer and the copolymer films were analyzed by using a JEOL JSM-6400 scanning electron microscope.  $M_n$  and  $M_w$  of the polymer obtained by chemical polymerization were determined by utilizing a PL-220 gel permeation chromatograph.

## **2.3. Procedure**

### **2.3.1. Synthesis of monomer**

#### **2.3.1.1. Synthesis of 1,4-di(2-thienyl)-1,4-butanedione (I)**

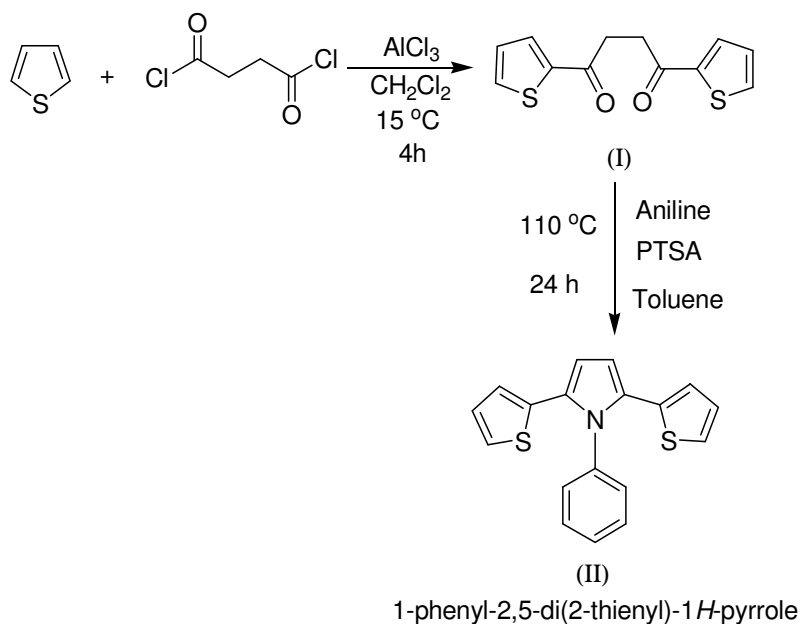
Among the various synthesis methods leading to 1,4-di(2-thienyl)-1,4-butanedione [85-92], the double Friedel-Crafts reaction, first proposed by Merz and Ellinger [91], was preferred. Thiophene and succinyl chloride were utilized as the reactants and aluminium chloride as the Lewis acid catalyst, since it is the most direct one-step procedure with good yields (78%). The synthetic route of 1,4-di(2-thienyl)-1,4-butanedione is shown in Scheme 2.1.

A solution of thiophene (0.12 mol, 9.61 ml) and succinyl chloride (0.05 mol, 5.51 ml) in  $\text{CH}_2\text{Cl}_2$  (30 ml) was added dropwise into a suspension of  $\text{AlCl}_3$  (16 g, 0.12 mol) in  $\text{CH}_2\text{Cl}_2$  (30 ml) at  $15^\circ\text{C}$ . The red mixture was stirred at  $15^\circ\text{C}$  for 4 h. This was then poured into a concentrated HCl (5 ml) and ice mixture. After stirring, a dark green organic phase separated out. The aqueous layer was extracted with  $\text{CH}_2\text{Cl}_2$  (2 x 30 mL). The combined organic layers were washed with saturated  $\text{NaHCO}_3$  and brine solutions and then dried over

MgSO<sub>4</sub>. After removal of the solvent under reduced pressure, the blue green solid was washed with ethanol and then dried.

### 2.3.1.2. Synthesis of 1-Phenyl-2,5-di(2-thienyl)-1H-pyrrole (II)

The monomer 1-phenyl-2,5-di(2-thienyl)-1H-pyrrole was synthesized from 1,4-di(2-thienyl)-1,4-butanedione and aniline in the presence of catalytical amounts of *p*-toluene-sulfonic acid (PTSA). A round-bottomed flask equipped with an argon inlet and mechanical stirrer was charged with 1.25 g (5 mmol) of the 1,4-di(2-thienyl)-1,4-butanedione, 7 mmol of aniline, *p*-toluenesulfonic acid (PTSA) (0.1 g, 0.58 mmol) and toluene (20 mL). The mixture was heated to reflux for 24 h under argon. Toluene was removed under reduced pressure. The residue obtained was purified by flash chromatography on silica gel [CH<sub>2</sub>Cl<sub>2</sub>/hexane, 1:1 (v:v)] . The 1-phenyl-2,5-di(2-thienyl)-1H-pyrrole was obtained at the solvent front. The synthetic route to the monomer is shown in Scheme 2.1.



**Scheme 2.1** Synthetic route of 1-phenyl-2,5-di(2-thienyl)-1*H*-pyrrole (PTP)

## 2.4. Synthesis of Conducting Polymers

### 2.4.1. Electrochemical Polymerization

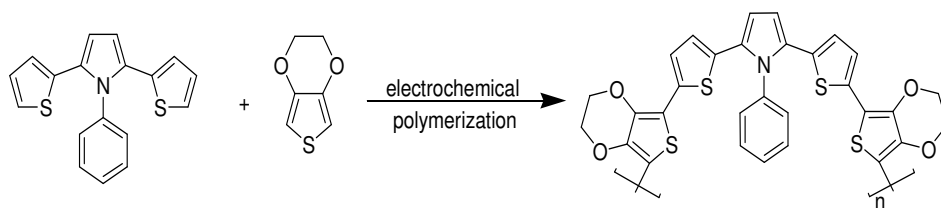
#### 2.4.1.1. Synthesis of Homopolymer of PTP

Polymerization of PTP was performed in the presence of 50 mg PTP, 0.1 M NaClO<sub>4</sub> / LiClO<sub>4</sub> in ACN in a single-compartment cell equipped with Pt working and counter electrodes and a Ag/Ag<sup>+</sup> reference electrode. Potentiodynamic electrolysis was run by sweeping the potential between -0.5V and +1.4 V with 500 mV.s<sup>-1</sup> scan rate. The free standing film that formed was

washed with ACN to remove unreacted monomer and excess  $\text{NaClO}_4/\text{LiClO}_4$  after electrolysis.

#### 2.4.1.2. Synthesis of Copolymer of PTP with 3,4-Ethylenedioxythiophene (EDOT)

For the synthesis of conducting copolymer P(PTP-co-EDOT), EDOT was used as comonomer (Scheme 2.2). 40 mg of PTP was dissolved in 0.1 M  $\text{NaClO}_4 / \text{LiClO}_4$  in ACN and 2  $\mu\text{L}$  of EDOT was introduced into a single compartment electrolysis cell. A three-electrode cell assembly was used where the working electrode was a platinum flake, the counter electrode was a platinum wire and a  $\text{Ag}/\text{Ag}^+$  wire was used as the reference electrode.

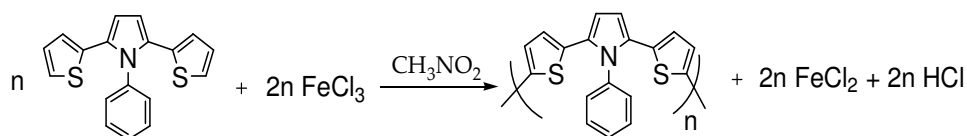


**Scheme 2.2** Copolymerization of PTP with EDOT

The copolymer was potentiodynamically synthesized by sweeping the potential between -0.5 V and +1.4 V with 500 mV/sec scan rate. The free standing film was washed with ACN in order to remove excess  $\text{NaClO}_4 / \text{LiClO}_4$  and unreacted monomer after the electrolysis.

## 2.4.2. Chemical Polymerization

Iron (III) chloride was used as the oxidant to perform a typical chemical polymerization of PTP (Scheme 2.3). Monomer ( $1 \times 10^{-3}$  M) was dissolved in nitromethane (15 mL) under a blanket of  $N_2$ . A solution of iron(III) chloride ( $2 \times 10^{-3}$  M) in nitromethane (5 mL) was added dropwise to the monomer solution. The reaction was carried out for 5 min. with constant stirring. The dark brown polymer was first washed with methanol, filtered and compensated with 30% NaOH. The resultant polymer was dried under vacuum for  $^1H$ -NMR analysis.



**Scheme 2.3** Oxidative chemical polymerization of PTP

## 2.5. Characterization of Conducting Polymers

### 2.5.1. Cyclic Voltammetry (CV)

Cyclic voltammetry is a useful tool for understanding a wide range of oxidation and reduction processes, particularly those occurring during the synthesis and redox reactions of conducting polymers.

In this technique, a potential is linearly scanned up to a switching potential and then reversed to its initial value (Figure 2.1 (a)). The current response is monitored as a function of the applied potential (Figure 2.1 (b)).

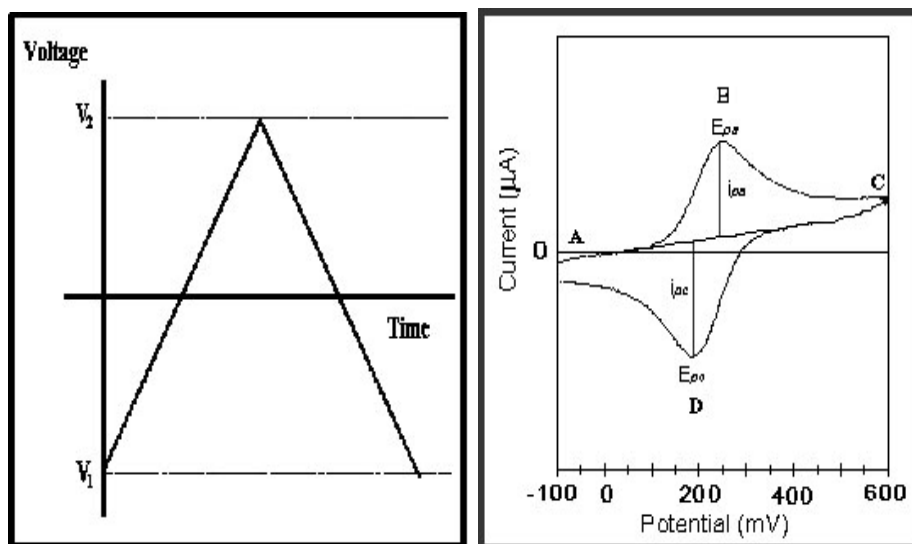


**Figure 2.1** (a) Triangular wave form (b) A cyclic voltammogram for a reversible redox reaction

Typically, the polymerization of electron rich monomers starts at low potentials, A where no redox reactions occur, followed by scanning in the anodic direction (Figure 2.1 (b)). At potential B, the electrode has sufficient oxidizing character to oxidize the monomer to its radical cation. The anodic current increase rapidly (B-C) until the concentration of the monomer at the electrode surface approaches zero, causing the current peak C, and then decay as the solution surrounding the electrode is depleted of monomer. Monomer oxidation is immediately followed by chemical coupling that affords oligomers in the vicinity of the electrode. Once these oligomers reach a certain length, they precipitate onto the electrode surface. The electroactivity of the polymer deposited onto the working electrode (WE) can be monitored by the appearance of a peak corresponding to the reduction of the oxidized polymer while scanning in the cathodic direction, D. The increase of the redox wave current of the polymer indicates the increase of polymer deposition on the working electrode.

The Randles-Sevcik equation states that the current at the peak potential is given by:

$$i_p = (2.69 \times 10^5)n^{3/2}AD^{1/2}CV^{1/2}$$

where  $n$  is the number of electrons transferred,  $A$  is the electrode surface area (in  $\text{cm}^2$ ),  $D$  is the diffusion constant ( $\text{cm}^2\text{s}^{-1}$ ),  $C$  is the bulk concentration ( $\text{mol}\cdot\text{cm}^{-3}$ ) and  $V$  is the scan rate ( $\text{Vs}^{-1}$ ). Therefore, for a diffusion-controlled system, the peak current is proportional to the square root of the scan rate.

The experimental setup of cyclic voltammetry consists of a working electrode, a counter electrode and a reference electrode (Figure 2.2).

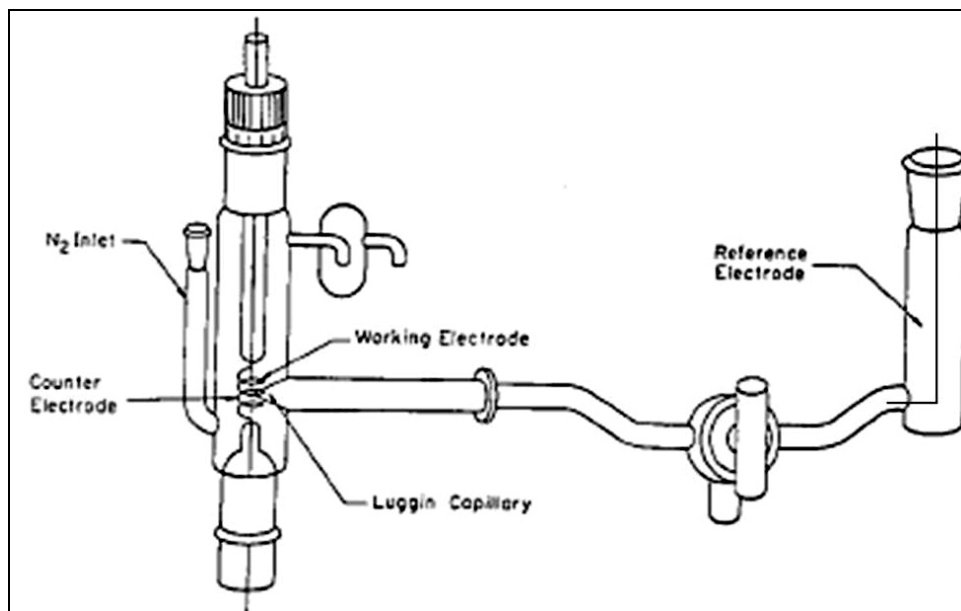


**Figure 2.2** Cyclic voltammetry cell

The desired potential is applied between a WE and a reference electrode (RE). WE is the electrode at which the electrolysis of interest take place. An

auxiliary (counter) electrode (CE) provides the current required to sustain the redox process developing at the working electrode. This arrangement prevents large currents from passing through the reference electrode, which could change its potential.

### 2.5.2. Conductivity Measurements

In order to determine the conductivity of polymer films, four probe conductivity measurements on the free standing films are performed.

This method has several advantages for measuring electrical properties of conducting polymers. First, the four probe technique eliminates errors caused by contact resistance, since two contacts measuring the voltage drop are different from the contacts applying the current across the sample. Secondly, this technique allows conductivity measurements over a broad range of applied currents.

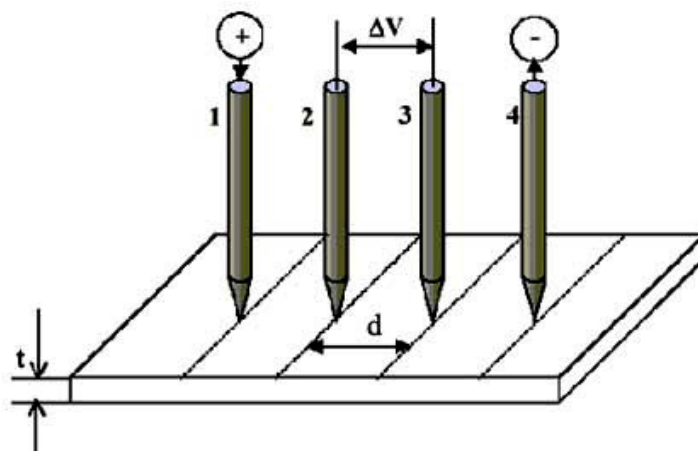


**Figure 2.3** Four-probe conductivity measurement setup [93]

Figure 2.3 demonstrates a simple four-probe measurement setup. The four osmium probes are aligned in a collinear geometry. A row of pointed

electrodes touches the surface of a polymer film taped on an insulating substrate. A known current  $I$  is injected at electrode 1 and collected at electrode 4, while the potential difference,  $\Delta V$  between contacts 2 and 3 is measured.

The four probe method allows for the contact points to be easily repositioned in various area of the film, thus allowing several conductivity measurements on the same sample.

Conductivity is calculated from the following equation,

$$\sigma = \frac{\ln 2}{\pi R t}$$

where  $R$  is the resistance of the sample, and  $t$  is the thickness.

### **2.5.3. Gel Permeation Chromatography (GPC)**

GPC is a widely used method for determining the molecular weight of a polymer. Most GPC results are reported as values relative to nearly monodisperse polystyrene standards. This technique provides number average ( $M_n$ ) and weight average ( $M_w$ ) molecular weight as well as molecular distribution (polydispersity,  $M_w/M_n$ ).

### **2.5.4. Scanning Electron Microscope (SEM)**

Scanning electron microscope is used to analyze the surface morphologies of the polymer films.

In a SEM, an electron beam interacts with the surface of a polymer. When electrons encounter a solid material, they may (i) pass through it without any interaction, (ii) undergo elastic scattering, i.e. change their direction without losing any energy, or (iii) undergo inelastic scattering, i.e.

change direction with an attendant loss of energy. A combination of these three phenomena will occur for a given sample material. As a result, backscattered electrons, secondary electrons, characteristic X-rays and several other types of radiation are generated during the process [94]. The inelastically scattered secondary electrons are collected by a detector to form an image of the specimen's surface morphology.

## 2.5.5. Electrochromic Properties of Conducting Polymers

### 2.5.5.1. Spectroelectrochemical Studies

In order to probe the electronic structure of the polymers and to examine the optical changes that occur during redox switching, optoelectrochemical analysis were carried out.

Polymer films were synthesized on a glass slide coated with indium tin oxide (ITO) from a 0.01M solution of monomer in  $\text{NaClO}_4/\text{LiClO}_4/\text{ACN}$ . The polymers were synthesized by potentiodynamic electrolysis. Then the polymer was reduced, washed with electrolyte solution to remove unreacted monomer.

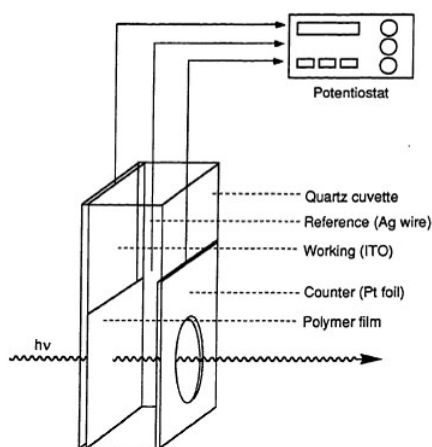


**Figure 2.4** In-situ optoelectrochemical analysis

For the spectroelectrochemical studies, the polymer film coated ITO was placed in a cuvette that is equipped with a reference electrode ( $\text{Ag}/\text{Ag}^+$ ) and a Pt wire counter electrode (Figure 2.4). This cell was then connected to a potentiostat, and the polymer was oxidized stepwise (normally in 0.2 V steps) while obtaining a spectrum at each potential. The results were then recorded as a graph of the extent of absorption as a function of wavelength.

### 2.5.5.2. Switching Studies

Long term switching studies were carried out to monitor absorbance changes with time during repeated potential stepping between bleached and colored states to obtain an insight into changes in the optical contrast (Figure 2.5). A square wave potential step method coupled with optical spectroscopy known as chronoabsorptometry was used to probe switching times and contrast in these polymers. Electrochromic contrast is often reported as percent transmittance change ( $\Delta T \%$ ) at a specified wavelength where the material has the highest optical contrast.

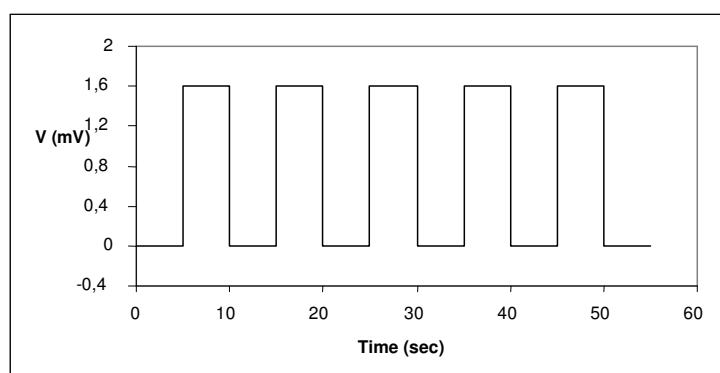


**Figure 2.5** Square wave voltammetry

In order to investigate their electrochromic switching properties, homopolymer and copolymer thin films were deposited on ITO-coated glass slides via potentiodynamic electrolysis in ACN/NaClO<sub>4</sub>/LiClO<sub>4</sub> solution that is 0.01 M in monomer. Switching properties of polymer films were investigated by the application of potential square wave technique with a residence time of 5 seconds between - 0.2 V and +1.0 V for the homopolymer, and between -0.5 V and +1.2 V for the copolymer.

### **2.5.5.3. Colorimetry**

Colorimetry was used to define the color of the polymers. The results were expressed in the CIE 1931 Lab color space. The relative luminance (*L*) and the a and b values were measured at the fully oxidized and reduced states of the homopolymer and copolymer. Color measurements were performed via a Coloreye XTH Spectrophotometer.

## **2.6. Electrochromic Device (ECD) Construction**

### **2.6.1. P(PTP)/PEDOT Electrochromic Device**

Electrochromic device of the homopolymer was constructed by using two complementary polymers, P(PTP) as the anodically and PEDOT as the cathodically coloring materials as deposited onto transparent electrodes. ECDs were prepared by arranging two electrochromic polymer films (one oxidized, the other neutral) facing each other separated by a gel electrolyte to allow ion transport (Figure 2.6).

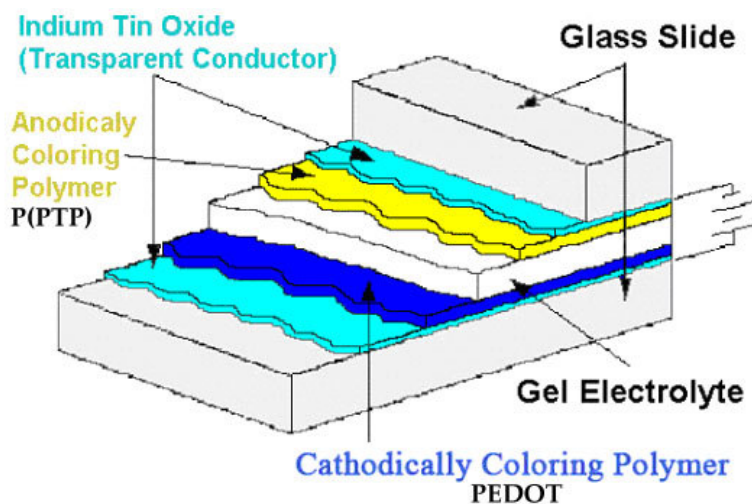


**Figure 2.6** Schematic illustration of dual type absorptive/transmissive type P(PTP)/PEDOT ECD configuration

P(PTP) was potentiodynamically deposited onto ITO sweeping between  $-0.5$  V and  $+1.4$  V in the presence of  $0.01$  M PTP in  $\text{NaClO}_4$  ( $0.1$  M) and  $\text{LiClO}_4$  ( $0.1$  M)/ACN solvent-electrolyte couple. The cathodically coloring polymer, poly(3,4-ethylenedioxythiophene) (PEDOT) was electrochemically deposited onto the ITO-coated glass from a  $0.1$  M solution of EDOT in  $0.1$  M ACN/ $\text{NaClO}_4$ / $\text{LiClO}_4$  at  $+1.5$  V versus  $\text{Ag}/\text{Ag}^+$ . Prior to construction, the charge capacities of the electrochemical layers were balanced. Thus, the residual charge formation during the coloring/bleaching was eliminated.

### 2.6.2. P(PTP-co-EDOT)/PEDOT

Copolymer of PTP was utilized as the anodically, and PEDOT as the cathodically coloring materials to construct electrochromic devices. Electrodeposition of P(PTP-co-EDOT) was potentiodynamically done by sweeping between  $-0.5$  V and  $1.4$  V in  $0.1$  M  $\text{NaClO}_4$  /  $\text{LiClO}_4$  in ACN.

PEDOT film was deposited onto ITO at +1.5 V vs. Ag/Ag<sup>+</sup> from a solution of EDOT in 0.1 M ACN/NaClO<sub>4</sub>/LiClO<sub>4</sub>.

### **2.6.3. Preparation of Gel Electrolyte**

A mixture of composition of NaClO<sub>4</sub>:LiClO<sub>4</sub>:ACN:PMMA:PC (1.5:1.5:70:7:20 percent respectively by weight) was used to prepare the gel electrolyte. PMMA was added into the solution after NaClO<sub>4</sub>:LiClO<sub>4</sub> was dissolved in ACN. Vigorous stirring and heating were applied to dissolve PMMA. Propylene carbonate (PC), as plasticizer, was introduced to the reaction medium when all of the PMMA was completely dissolved. The mixture was stirred and heated to roughly 70°C until the highly conducting transparent gel was produced.

## **2.7. Characterization of Electrochromic Devices**

### **2.7.1. Spectroelectrochemistry Studies of Electrochromic Devices**

Varian Cary 5000 UV-Vis-NIR and Agilent 8453 UV-Vis spectrophotometers were used to characterize the optical properties of electrochromic devices (ECDs). A device without the active polymer layer was used as the reference during spectroscopic studies. Applied potentials were delivered via a potentiostat where the counter and the reference electrodes were short cut and working electrode was connected to anodically coloring polymer layer.

Optoelectrochemical analyses of the devices were obtained by sequentially stepping the applied potential of the polymer. The alternation of the color was observed upon stepwise increase of the potential from -0.6 V to 1.6 V for P(PTP)/PEDOT while measuring the absorbance as a function of wavelength.

Spectroelectrochemical study of P(PTP-co-EDOT)/PEDOT device was carried out by varying the voltage between -0.8 V and + 1.8 V and absorbance was measured as a function of wavelength.

### **2.7.2. Switching Properties of Electrochromic Devices**

A square-wave potential step method coupled with optical spectroscopy was used to investigate the electrochromic switching properties of ECDs. The potential was stepped between -0.6 V and +1.6 V with a residence time of 5 s for P(PTP)/PEDOT.

The P(PTP-co-EDOT)/PEDOT was switched between -0.8 V and + 1.8 V with a residence time of 5 s to probe switching time and optical contrast in the device.

### **2.7.3. Stability of Electrochromic Devices**

The stability of the devices for long term switching between oxidized and neutral states was evaluated by CV studies. Continuous cycling of the applied potential between -0.6 V and +1.6 V for P(PTP)/PEDOT with  $500\text{mVs}^{-1}$  was performed to analyze the stability of device. The P(PTP-co-EDOT)/PEDOT was repeatedly switched between -0.8 V and +1.8 V at  $500\text{mV}\cdot\text{s}^{-1}$  to monitor its stability.

### **2.7.4. Open Circuit Memory**

The color persistence in P(PTP)/PEDOT was examined by polarizing the device in the fully reduced/ oxidized states by an applied pulse (-0.6

V/+1.6V, respectively) for 1 s and then holding at open circuit conditions for 200 s.

In order to explore the color persistence in P(PTP-co-EDOT)/PEDOT, the device was polarized in its two extreme states by an applied pulse for 1s and then holding at open circuit conditions for 200 s. Simultaneously, the optical spectrum as a function of time at open circuit condition was monitored.

## CHAPTER III

### RESULTS AND DISCUSSION

#### 3.1. Characterization by $^1\text{H}$ -NMR and $^{13}\text{C}$ - NMR Spectroscopy

$^1\text{H}$ -NMR and  $^{13}\text{C}$ -NMR spectra of the monomer (PTP) and  $^1\text{H}$ -NMR of the polymer were investigated with  $\text{CDCl}_3$  as the solvent and chemical shifts ( $\delta$ ) are given relative to tetramethylsilane as the internal standard. Results are summarized below:

Pale green powder; mp 180 °C;  $^1\text{H}$ -NMR spectrum of monomer (Figure 3.1):  $\text{C}_{18}\text{H}_{13}\text{NS}_2$ ,  $\delta_{\text{H}}$  ( $\text{CDCl}_3$ ): 6.54 (2H, d,  $J=4$  Hz, thienyl-*Hc*), 6.57 (2H, s, pyrrolyl-*Hd*), 6.83 (2H, dd,  $J=4$  Hz, thienyl-*Hb*), 7.08 (2H, d,  $J=5$  Hz, thienyl-*Ha*), 7.34 (1H, d,  $J=8$  Hz, phenyl- *Hg*), 7.42-7.47 (4H, m, phenyl-*He,f*).

$^{13}\text{C}$ -NMR spectrum of the monomer (Figure 3.2):  $^{13}\text{C}$ -NMR ( $\delta$ ,ppm): 110.2, 125.0, 125.3, 128.1, 129.4, 130.0, 130.4, 130.9, 135.9, 139.6.

$^1\text{H}$ -NMR spectrum of polymer (Figure 3.3):  $\text{C}_{18}\text{H}_{13}\text{NS}_2$ ,  $\delta_{\text{H}}$  ( $\text{CDCl}_3$ ): 6.20-6.30 (2H, broad s, thienyl-*Hc*), 6.30-6.50 (2H, broad s, pyrrolyl-*Hd*), 6.56-6.67 (2H, broad s, thienyl-*Hb*), 6.73-6.83 (2H, broad s, thienyl-*Ha*), 7.08-7.45 (3H, broad m, phenyl-*He,f,g*). The decrease in the intensity of  $\text{H}_a$  confirms the polymerization through position 2 of thiophene moiety of the monomer.

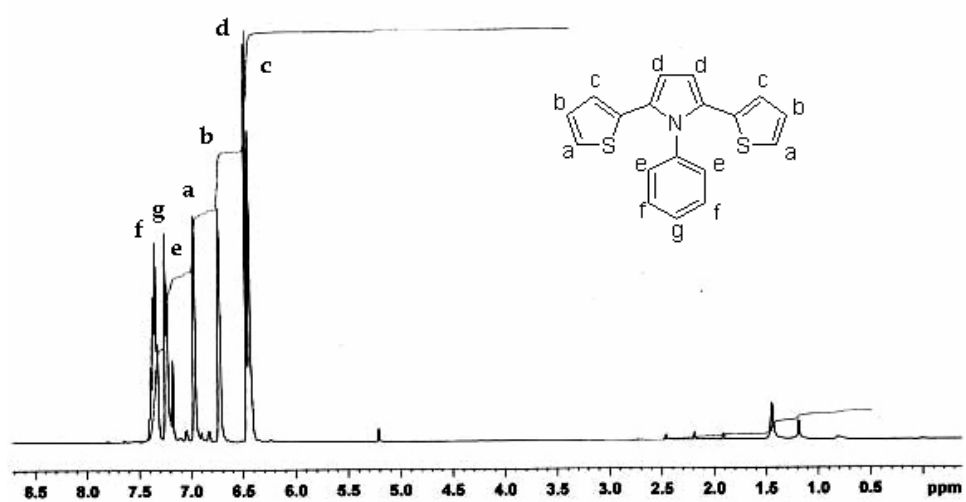


Figure 3.1  $^1\text{H-NMR}$  spectrum of PTP

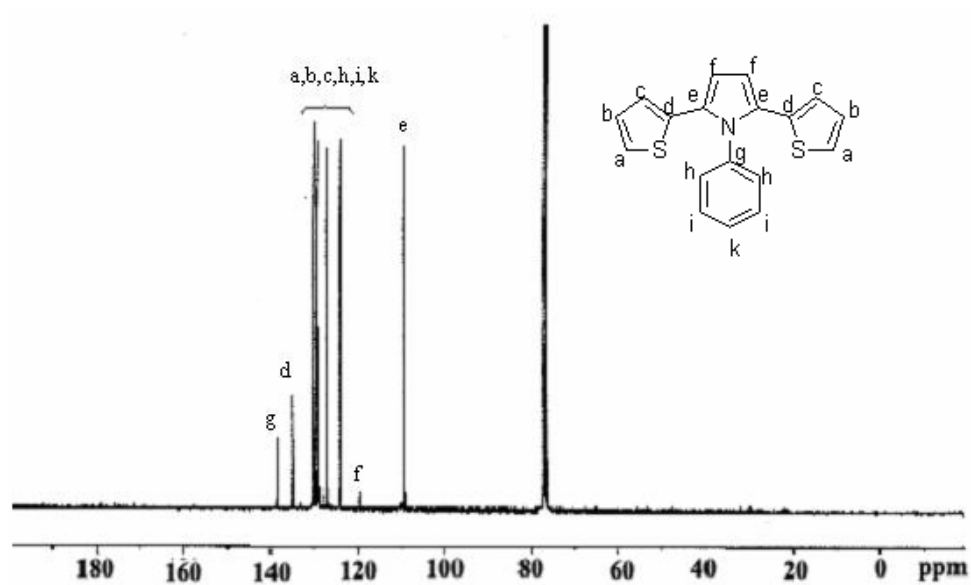
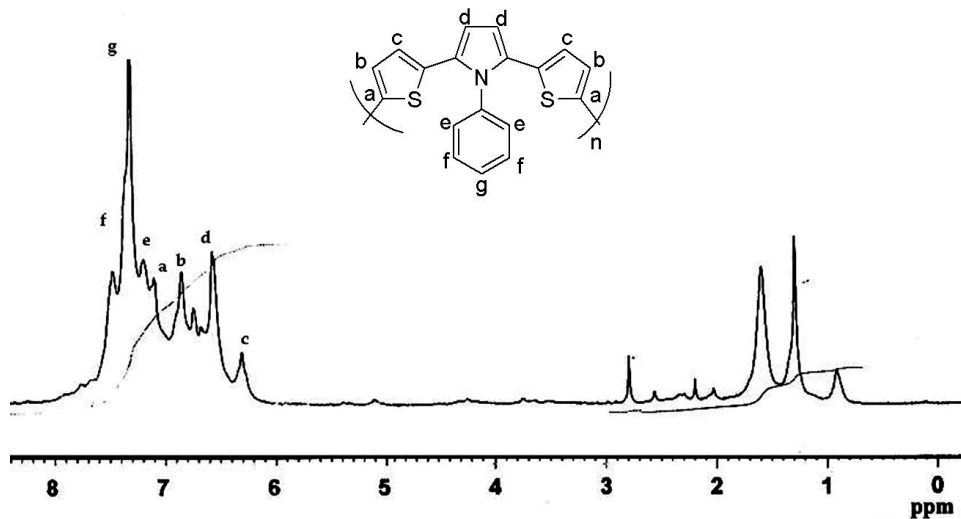


Figure 3.2  $^{13}\text{C-NMR}$  spectrum of PTP



**Figure 3.3**  $^1\text{H-NMR}$  spectrum of the chemically synthesized P(PTP)

### 3.2. FTIR Spectra

FTIR spectrum (Figure 3.4 (a)) of the PTP indicated the following absorption peaks:  $3097\text{ cm}^{-1}$  (aromatic C–H),  $3033\text{ cm}^{-1}$  (C–H $_{\alpha}$  stretching of thiophene),  $1496\text{--}1340\text{ cm}^{-1}$  (aromatic C=C, C–N stretching due to pyrrole and benzene),  $1045\text{ cm}^{-1}$  (C–H in plane bending of benzene),  $771\text{ cm}^{-1}$  (C–H $_{\alpha}$  out of plane bending of thiophene) and  $697\text{ cm}^{-1}$  (monosubstituted benzene).

FTIR spectrum (Figure 3.4 (b)) of electrochemically synthesized P(PTP) showed the characteristic peaks of the monomer. The peaks related to C–H $_{\alpha}$  stretching of thiophene disappeared completely. The new broad band at around  $1641\text{ cm}^{-1}$  was due to polyconjugation. The strong absorption peak at  $1121$  and  $668\text{ cm}^{-1}$  were attributed to the incorporation  $\text{ClO}_4^-$  ions into the polymer film during doping process.

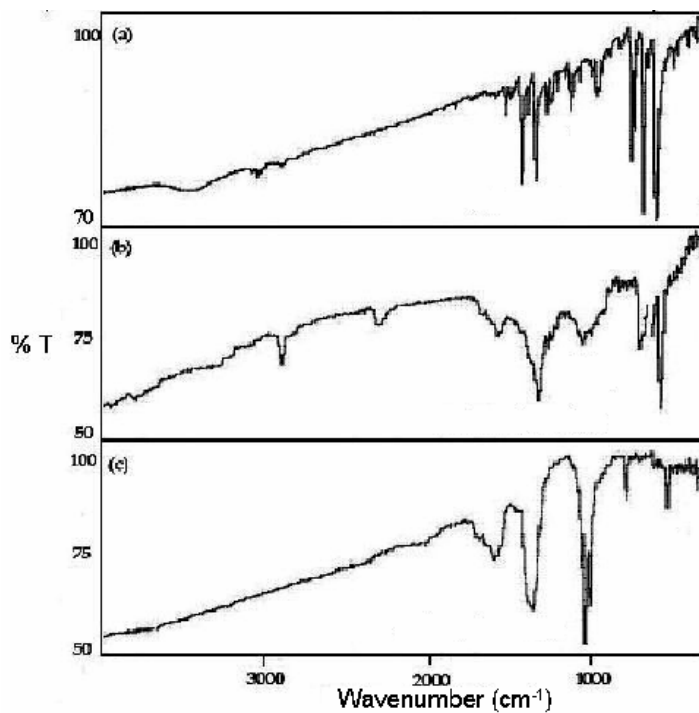


**Figure 3.4** FTIR spectra of (a) PTP, (b) electrochemically synthesized P(PTP), and (c) chemically synthesized P(PTP)

Most of the characteristic peaks of the monomer PTP remained unperturbed upon chemical polymerization (Figure 3.4 (c)). Absorption bands of the monomer at  $3033\text{ cm}^{-1}$  and  $771\text{ cm}^{-1}$  arising from C–H<sub>α</sub> stretching of thiophene moiety disappeared completely. This is an evidence of the polymerization from 2,5 positions of thiophene moiety of the monomer. Two new bands related to C–H<sub>α</sub> out-of-plane bending of 2,5 disubstituted thiophene and C–S stretching appeared at  $839$  and  $632\text{ cm}^{-1}$ , respectively. The broad band observed at around  $1613\text{ cm}^{-1}$  points to the presence of polyconjugation and the new peak at  $682\text{ cm}^{-1}$  indicates the presence of the dopant ion. Results of the FTIR studies clearly indicated homopolymerization of the monomer.

FTIR spectrum (Figure 3.5) of electrochemically synthesized P(PTP-co-EDOT) showed the characteristic peaks of the monomer (PTP) and comonomer (EDOT).

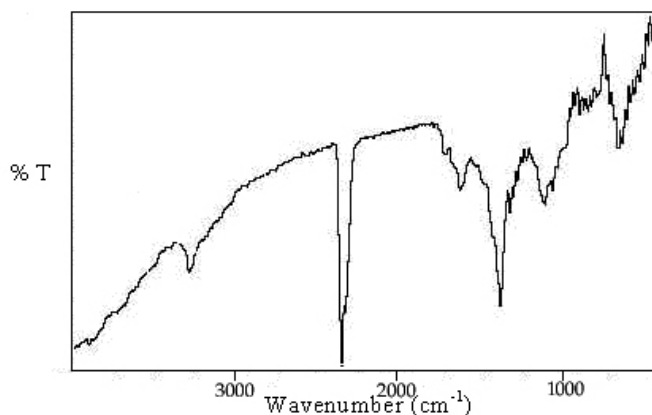


**Figure 3.5** FTIR spectrum of P(PTP-co-EDOT)

The following absorption peaks of the monomer remained unperturbed upon copolymerization:  $1512\text{ cm}^{-1}$  (conjugated cyclic C=N stretching),  $980\text{ cm}^{-1}$  (1,2,5 trisubstituted pyrrole) and  $697\text{ cm}^{-1}$  (monosubstituted benzene). The characteristic peaks of the comonomer EDOT at  $2324\text{ cm}^{-1}$  (aliphatic C-C),  $1633\text{ cm}^{-1}$  (C-O stretching) were observed in FTIR spectrum of electrochemically synthesized P(PTP-co-EDOT). Absorption bands of the monomer and comonomer at  $3020\text{ cm}^{-1}$  and  $771\text{ cm}^{-1}$  arising from C-H<sub>α</sub> stretching of thiophene moiety disappeared completely. This is an evidence of the polymerization from 2,5 positions of thiophene moiety of the monomer and EDOT. The strong absorption peak at  $1118\text{ cm}^{-1}$  was attributed to the incorporation ClO<sub>4</sub><sup>-</sup> ions into the polymer film during doping process. Results of the FTIR studies clearly indicated copolymerization of the PTP with EDOT.

### 3.3. Cyclic Voltammograms

Oxidative electrochemical polymerization of PTP was carried out in acetonitrile with 0.1 M  $\text{LiClO}_4/\text{NaClO}_4$  as the supporting electrolyte. Figure 3.6 shows the first 7 scans for the anodic electropolymerization of a solution of PTP on an ITO electrode by cyclic voltammetry at  $500 \text{ mV}\cdot\text{s}^{-1}$ .

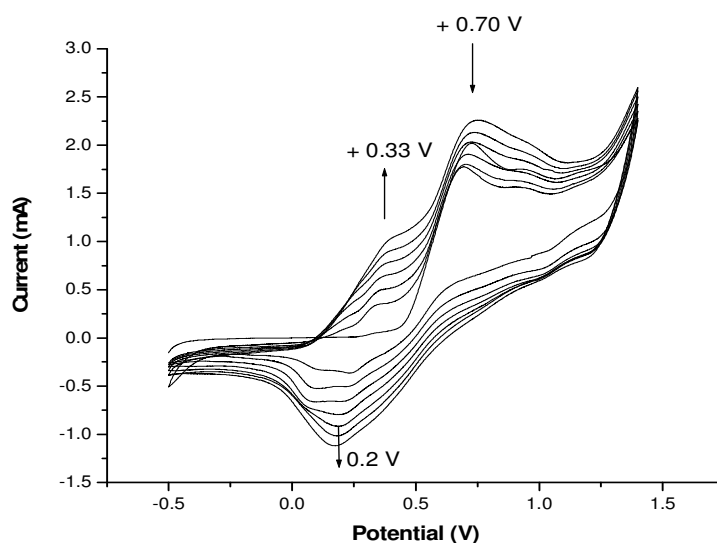


**Figure 3.6** Cyclic voltammogram of P(PTP)

This monomer revealed an irreversible oxidation peak at + 0.70 V whose intensity decreases upon consecutive cycles along with the leakage of oligomers. A well-defined redox system builds rapidly at about + 0.33 V vs  $\text{Ag}/\text{Ag}^+$  with a fast electrodeposition rate. Upon consecutive cycles, there was a gradual increase in the current intensity, indicating continuous film formation.

The oxidation/reduction behavior of the PTP through copolymerization in the presence of EDOT was investigated via cyclic voltammetry. Oxidative electropolymerization of PTP with EDOT was carried out in acetonitrile with 0.1 M NaClO<sub>4</sub> / LiClO<sub>4</sub> as supporting electrolyte. The oxidation peak of PTP drastically shifted to + 0.74 V when EDOT was added into the system (Figure 3.7 (a)). When CV of P(PTP-co-EDOT) is compared with the voltammogram of pristine EDOT (Figure 3.7 (b)), the redox peaks are not at the same positions (pure PEDOT- E<sub>p,a</sub>: 0.17 V, E<sub>p,c</sub>: -0.88 V).

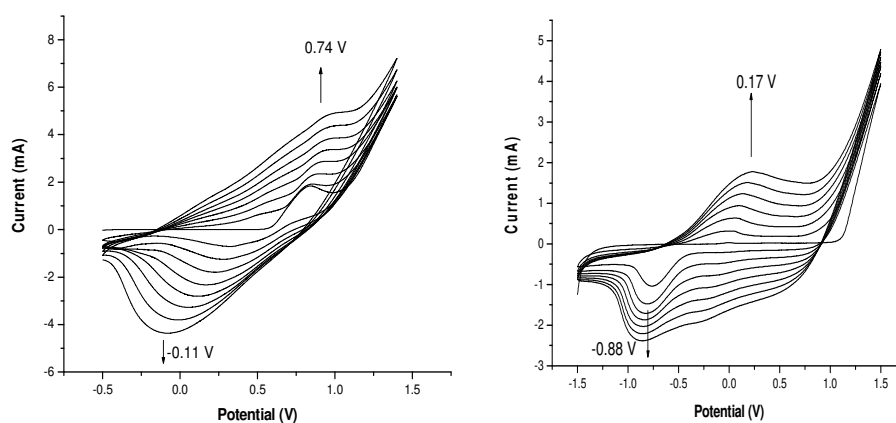


**Figure 3.7** Cyclic voltammograms of (a) P(PTP-co-EDOT), (b) pristine PEDOT

According to these observations it is considered that both EDOT and PTP were oxidized within the same potential range and radical cations of both monomers formed almost at the same time on the working electrode surface where they react with each other. Both the current increase in the increments between consecutive cycles and the redox potentials of the copolymer compare to those of pure PEDOT and P(PTP) are different. These differences are known to be an indication for the reaction between EDOT and the thiophene moiety of PTP, resulting copolymer formation.

### 3.4. Conductivities of the films

The conductivities of the solution and the electrode sides were measured by the standard four-probe technique. When the electrode side and the solution side conductivities were compared, equal conductivities were observed almost in each case. This reveals the homogeneity of the films. The conductivity of the P(PTP-co-EDOT) is found to be  $3 \times 10^{-2} \text{ S.cm}^{-1}$ . The conductivities of pristine PEDOT and P(PTP) are  $1 \times 10^{-2} \text{ S.cm}^{-1}$  and  $2.3 \times 10^{-5} \text{ S.cm}^{-1}$ , respectively. It is observed that the conductivity increased by about 1000 orders of magnitude upon copolymerization. This is expected since the presence of EDOT increases the conjugation in pristine P(PTP) chains.

**Table 3.1** Conductivities of Films of Polymers ( $\text{S.cm}^{-1}$ )

Polymer	Conductivity ( $\text{S.cm}^{-1}$ )
P(PTP)	$2.3 \times 10^{-5}$
P(PTP-co-EDOT)	$3 \times 10^{-2}$
PEDOT	$1 \times 10^{-2}$

### 3.5. Morphologies of the films

Surface morphologies of polymers were investigated by Scanning Electron Microscopy. SEM micrograph of the solution side of P(PTP) film showed a droplet structure (Figure 3.8 (a)). Globules like droplets were observed on the solution side of P(PTP-co-EDOT) film (Figure 3.8 (b)).

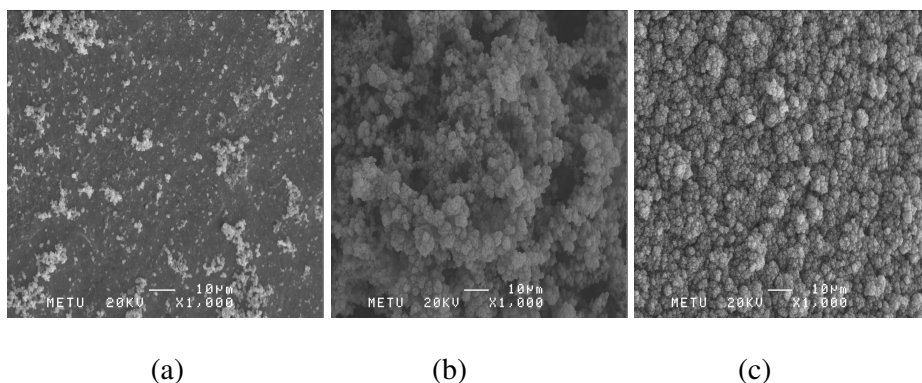


**Figure 3.8** SEM micrographs of (a) P(PTP), (b) P(PTP-co-EDOT) (c) PEDOT

SEM micrograph of P(PTP-co-EDOT) implies that the synthesized polymer was good in film forming, exhibiting homogeneous structure. The surface morphology of the solution side of P(PTP-co-EDOT) showed microstructures less compact than that of the pristine PEDOT (Figure 3.8 (c)). Surface morphology of the solution side of P(PTP-co-EDOT) was different from that of PEDOT, clearly indicating the presence of a different species than for both homopolymers.

### 3.6. Gel Permeation Chromatography (GPC)

The weight average and number average molecular weights of chemically synthesized P(PTP) were determined by GPC. The results of GPC studies are given in Table 3.2. The polydispersity ( $PD=M_w/M_n$ ) of P(PTP) was found as 1.14 which means almost all polymer chain have the same number of repeating units. The number of repeating units was calculated as 26.

**Table 3.2** GPC Results

<b>Mn</b>	7.2 x10 <sup>3</sup> g/mol
<b>Mw</b>	8.2 x10 <sup>3</sup> g/mol
<b>PD</b>	1.14

### **3.7. Investigation of Electrochromic Properties of Polymers**

#### **3.7.1. Spectroelectrochemistry**

Spectroelectrochemistry experiments were done to reveal key properties of conjugated polymers, such as the band gap ( $E_g$ ) and intergap states that appear upon doping. Spectroelectrochemical analysis of P(PTP) were studied to clarify electronic transitions upon doping the polymer. The film was deposited on ITO via potentiodynamic electrochemical polymerization of PTP in the presence of  $\text{NaClO}_4 / \text{LiClO}_4 / \text{ACN}$  at -0.5 V and +1.4 V. P(PTP) coated ITO was investigated by UV-Vis spectroscopy in the same but monomer free electrolytic system by switching between -0.2 V and +1.0 V with incremental increase in applied potential (Figure 3.9).

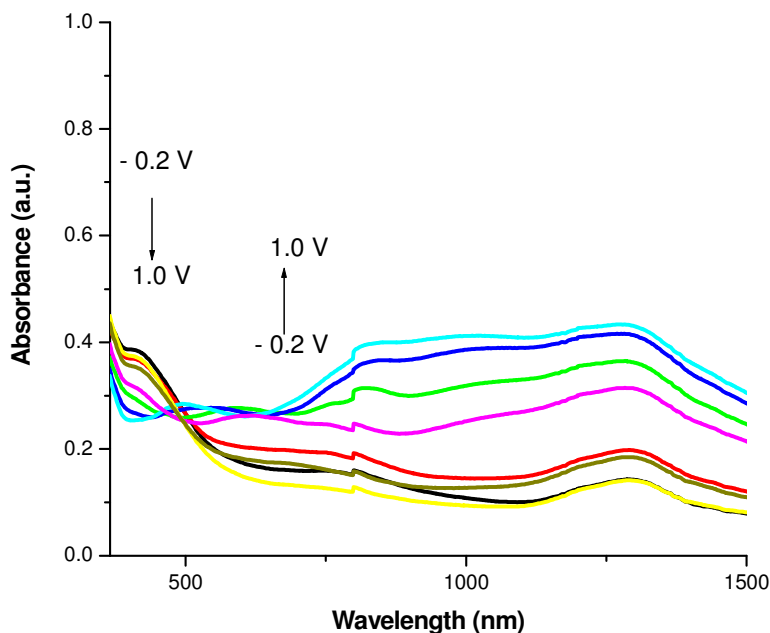


**Figure 3.9** Spectroelectrochemical spectrum of P(PTP) with applied potentials between -0.2 V and + 1.0 V in ACN/NaClO<sub>4</sub>/LiClO<sub>4</sub> (0.1 M)

There was a gradual decrease in the peak intensity of the  $\pi$ - $\pi^*$  transition upon increasing the applied voltage (Figure 3.10). The onset energy for the  $\pi$ - $\pi^*$  transition which is called the electronic band gap ( $E_g$ ), was found to be 2.2 eV and  $\lambda_{\text{max}}$  was 413 nm. Upon applying voltage, formation of charge carrier bands were observed. Thus, appearance of peaks at around 600 and 900 nm could be attributed to the evolution of polaron and bipolaron bands, respectively (Figure 3.10). This resulting UV-Vis spectrum confirmed the typical bipolaronic nature of charge carriers.

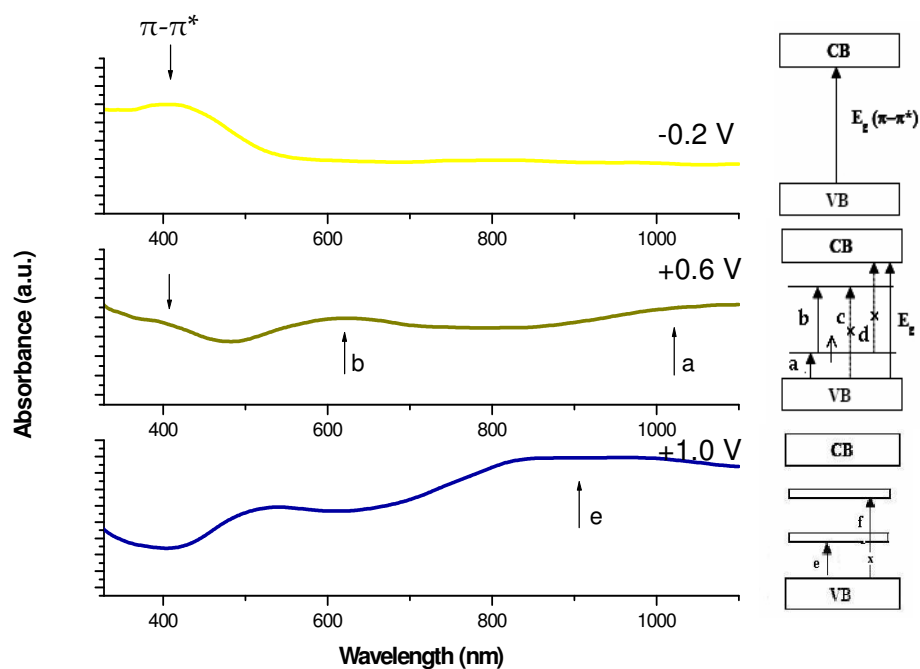


**Figure 3.10** Polaron and bipolarons in non-degenerate ground state P(PTP): band diagrams for (a) neutral , (b) polaron and (c) bipolaron

Figure 3.11 presents the spectroelectrochemistry of P(PTP-co-EDOT) showing that the absorbance of the  $\pi$ - $\pi^*$  transition in the neutral state ( - 0.5 V) is claret red, displaying a maximum at 480 nm. The electronic bandgap, calculated from the onset of the  $\pi$ - $\pi^*$  transition, is 1.9 eV. Upon oxidation, the  $\pi$ - $\pi^*$  transition is depleted at the expense of a peak at about 600 nm , corresponding to the charge carrier (radical cations) and producing a blue color at +1.2 V versus  $\text{Ag}/\text{Ag}^+$  .

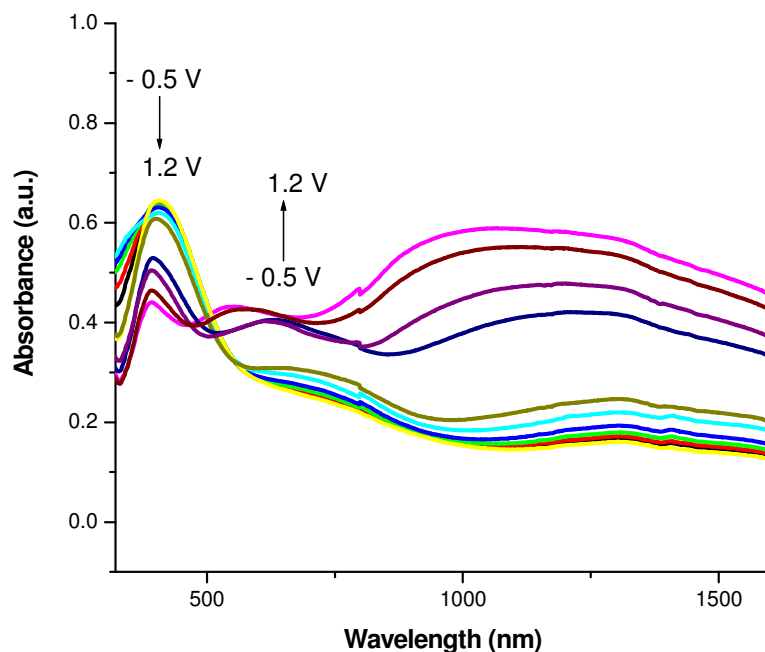


**Figure 3.11** Spectroelectrochemical spectrum of P(PTP-co-EDOT) with applied potentials between -0.5 V and +1.2 V in ACN/NaClO<sub>4</sub>/LiClO<sub>4</sub> (0.1 M)

### 3.7.2. Electrochromic Switching

Electrochromic switching studies were done to monitor the ability of a polymer to switch reversibly and rapidly between its extreme states. A square-wave potential step method coupled with optical spectroscopy was used to investigate switching time and contrast in the polymer.

In this double potential step experiment for P(PTP), the potential was set at an initial value (-0.2 V) for a set period of time (5s) and was stepped to a second potential (+1.0 V) for the same period of time, before being switched back to the initial potential again (Figure 3.12). Electrochromic contrast was reported as a percent transmittance change ( $\Delta T$  %) at 413 nm where the

electrochromic material has the highest optical contrast. The contrast was measured as the difference between T % in the reduced and oxidized forms and  $\Delta T$  % was noted as 27 %. Results showed that time required to reach 95 % of ultimate  $\Delta T$  % was 1.7 s.

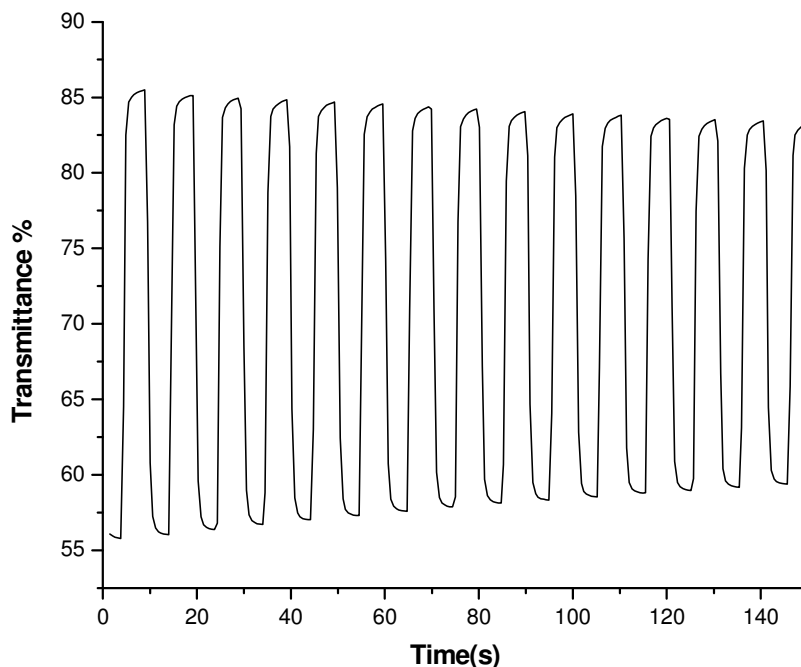


**Figure 3.12** Electrochromic switching, optical absorbance change monitored at 418 nm for P(PTP) between -0.2 V and + 1.0 V

The electrochromic switching properties of P(PTP-co-EDOT) was investigated by switching a film between -0.5 V and + 1.2 V versus Ag / Ag<sup>+</sup> in 0.1 M NaClO<sub>4</sub> / LiClO<sub>4</sub> in ACN. Figure 3.13 shows the behavior of this film during potential switching at 480 nm yielding a contrast ratio of about 8 % ( $\Delta T$  %). Switching speed reported as the time required for the coloring/bleaching process of an EC material was 1.7 s.

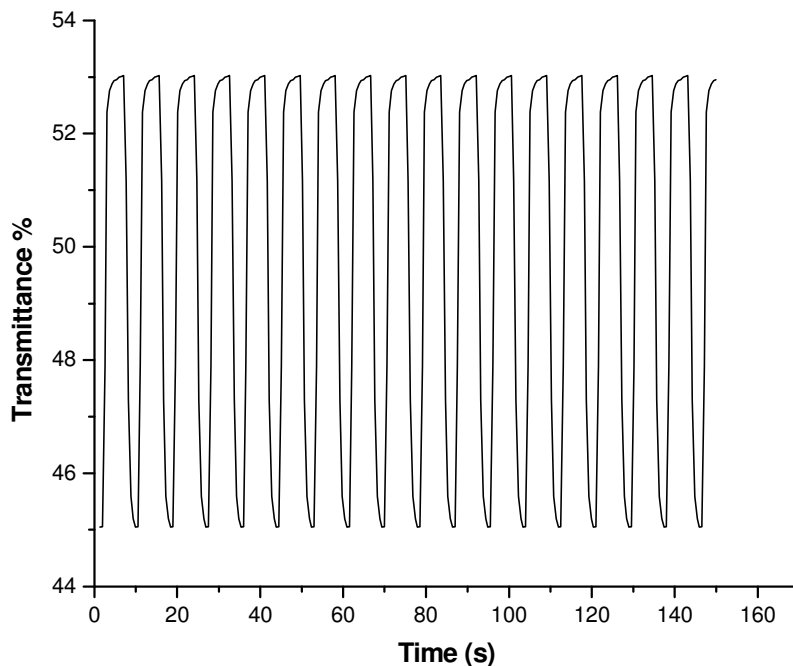


**Figure 3.13** Electrochromic switching, optical absorbance change monitored at 480 nm for P(PTP-co-EDOT) between -0.5V and +1.2 V

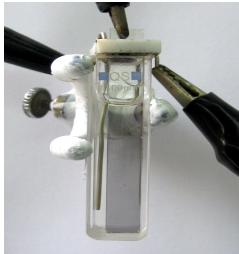
### 3.7.3. Colorimetry of Polymers

The color of the film switches from yellow in the reduced state (-0.2 V) to blue in the oxidized state (1.0 V). The relative luminance ( $L$ ) and the  $a$  and  $b$  values (Table 3.3) were measured at the fully oxidized and reduced states of P(PTP).

The copolymer revealed completely different spectroelectrochemical behavior in comparison to both of the homopolymers, where synergy was achieved due to copolymerization. It was important to note that only the copolymer displayed distinct multichromism. The color coordinates of the

copolymer were also determined by colorimetry in order to have an accurate objective measurement (Table 3.4).

**Table 3.3** Electrochromic properties of P(PTP)

	
<p>(-0.2 V)            L = 56            a = -12            b = -8</p>	<p>(1.0 V)            L = 68            a = -14            b = 14</p>

**Table 3.4** Electrochromic properties of P(PTP-co-EDOT)

		
<p>(- 0.5 V)            L= 47            a= 17            b= 28</p>	<p>(0.3 V)            L= 61            a= -24            b= 48</p>	<p>(1.0 V)            L= 48            a= -5            b= -7</p>

### 3.8. Characterization of Electrochromic Devices (ECDs)

#### 3.8.1. Spectroelectrochemistry of ECDs

Spectroelectrochemical studies were carried out to examine the optical properties of the ECDs that occur upon doping or dedoping, and to obtain information on the electronic structure. Optoelectrochemical spectrum of P(PTP)/PEDOT device as a function of applied potential is given in Figure 3.14. The alternation of the color from yellow to blue was observed upon stepwise increase of the potential from -0.6 V to 1.6 V. The UV-Vis spectroscopy results implied that anodically coloring material, P(PTP), dominant in the features of the device, reveals yellow color at -0.6 V. The maximum absorption was at 386 nm due to  $\pi$ - $\pi^*$  transitions of the electrochromic layer, P(PTP). At this potential, cathodically coloring material, PEDOT, was in its oxidized state revealing a transparent sky blue color. Application of further positive potential caused oxidation of P(PTP) layers and decrease in the intensity of the peak due to  $\pi$ - $\pi^*$  transitions. The device starts to reflect the PEDOT dominance at potentials beyond + 0.8 V. The alternation of the color to blue and evaluation of a new peak at around 606 nm due to the  $\pi$ - $\pi^*$  transition of PEDOT itself was observed while the intensity of the  $\pi$ - $\pi^*$  transition of anodically coloring electrochromic layer was decreasing. The spectral behavior of the absorption/transmission type electrochromic device could be considered as the rough summation of spectral signatures of the two active layers.

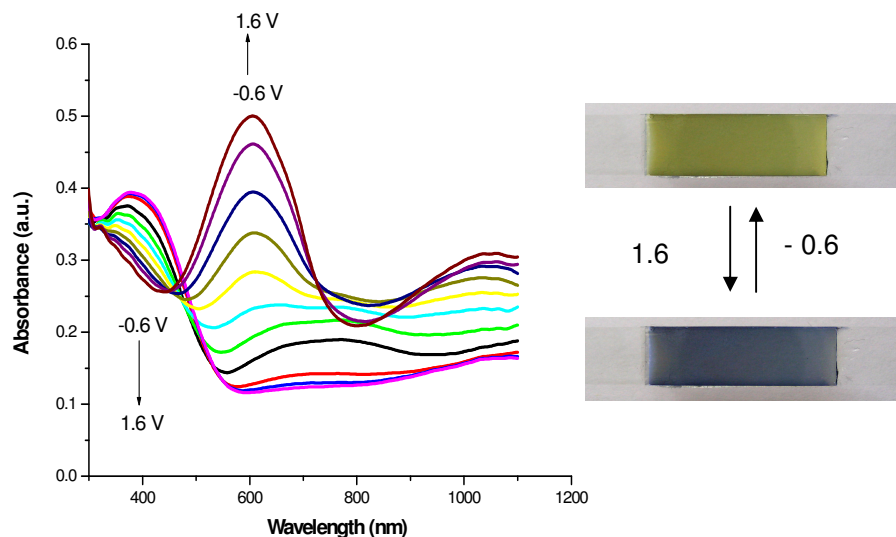


**Figure 3.14** Spectroelectrochemical spectrum of P(PTP)/PEDOT device with applied potentials between -0.6 and +1.6 V

Optoelectrochemical spectrum of P(PTP-co-EDOT)/PEDOT device as a function of applied potential is given in Figure 3.15. There was a maximum absorption at 545 nm due to the  $\pi$ - $\pi^*$  transition of the electrochromic P(PTP-co-EDOT) layer at  $-0.8$  V. Upon application of positive potential, P(PTP-co-EDOT) layer started to oxidize and the intensity of the peak due to the  $\pi$ - $\pi^*$  transition decreased. There appears to be a second intense absorption at around 600 nm due to the formation of a charge carrier band. At potentials beyond  $+1.0$  V, the device starts to reflect the PEDOT dominance, shown by the alternation of the color to blue and evolution of a new peak at around 635 nm due to the  $\pi$ - $\pi^*$  transition of PEDOT.

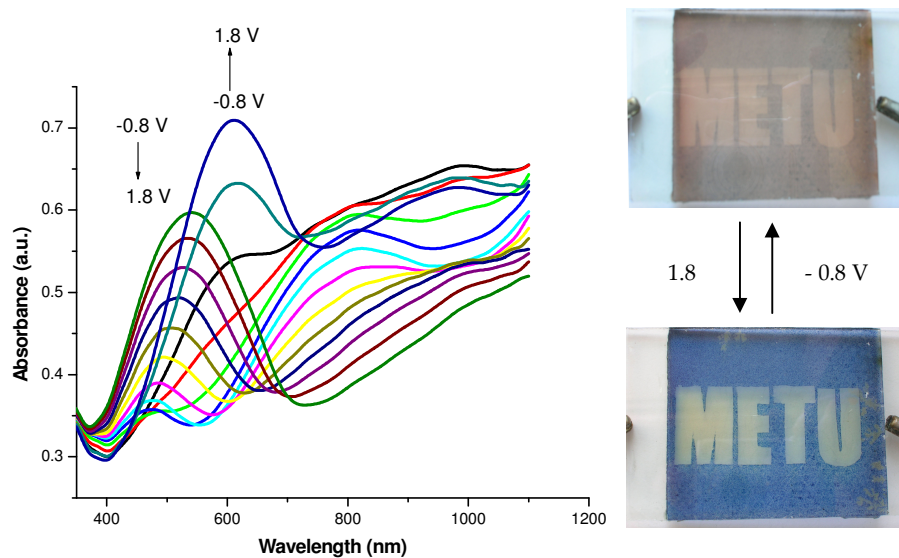


**Figure 3.15** Spectroelectrochemical spectrum of P(PTP-co-EDOT)/PEDOT device with applied potentials between -0.8 and +1.8 V

The luminance (L) and the a (hue), b (saturation) values of the devices (Table 3.5) were measured at bleached and colored state. The color of P(PTP)/PEDOT device switches from yellow to blue and P(PTP-co-EDOT)/PEDOT switched between claret red and blue.

**Table 3.5** Colorimetry data for P(PTP)/PEDOT and P(PTP-co-EDOT)/PEDOT ECDs

Electrochromic Device	Color	L	a	b
P(PTP)/PEDOT	Blue ( 1.6 V)	14	28	-54
	Yellow (-0.6 V)	61	-4	26
P(PTP-co-EDOT)/PEDOT	Blue (1.8 V)	46	-4	-35
	Claret red(- 0.8V)	56	6	-5

### 3.8.2 Switching of ECDs

The response time needed to perform switching between the two colored states and the device's stability during repeated cycles were evaluated by using double potential step chronoabsorptometry.

The time required to change the color of P(PTP)/PEDOT device from yellow to blue was determined by kinetic studies while applying the potential step square wave form with a residence time of 5s. A UV-Vis spectrophotometer was used to measure the % transmittance (T %) at the wavelength of maximum contrast. The optical contrast ( $\Delta T$  %) was monitored as the difference in T % between the reduced and oxidized forms ( $T_{\text{red}} - T_{\text{ox}}$ ).

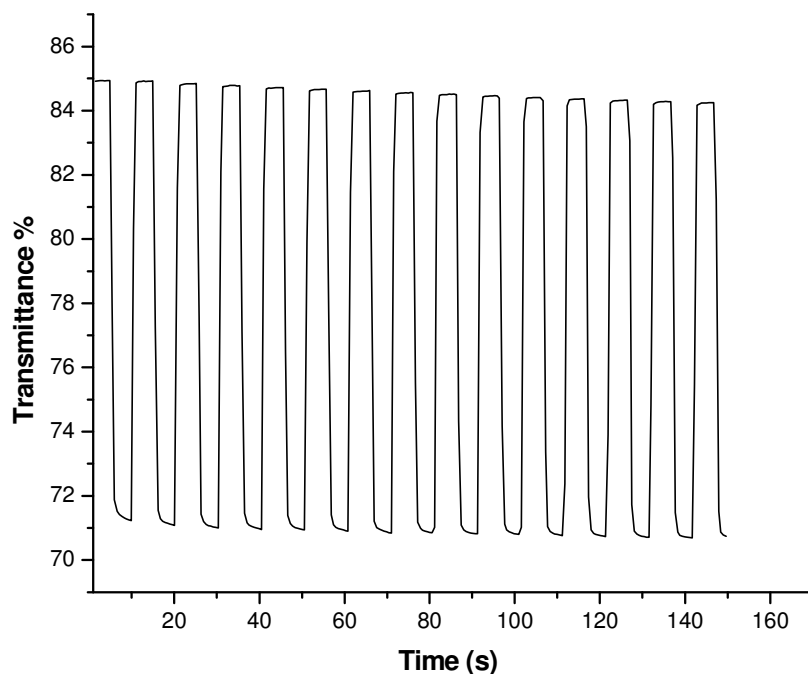


**Figure 3.16** Electrochromic switching, optical absorbance change monitored at 386 nm for P(PTP)/PEDOT device between -0.6 V and 1.6 V

Figure 3.16 demonstrates the transmittance change at 386 nm (wavelength of maximum contrast) while the potential was stepped between -0.6 V and +1.6 V. The optical contrast was found to be 13 % for P(PTP)/ PEDOT device. The time required to reach 95 % of the ultimate  $\Delta T$  % was 2.1 s for the device.

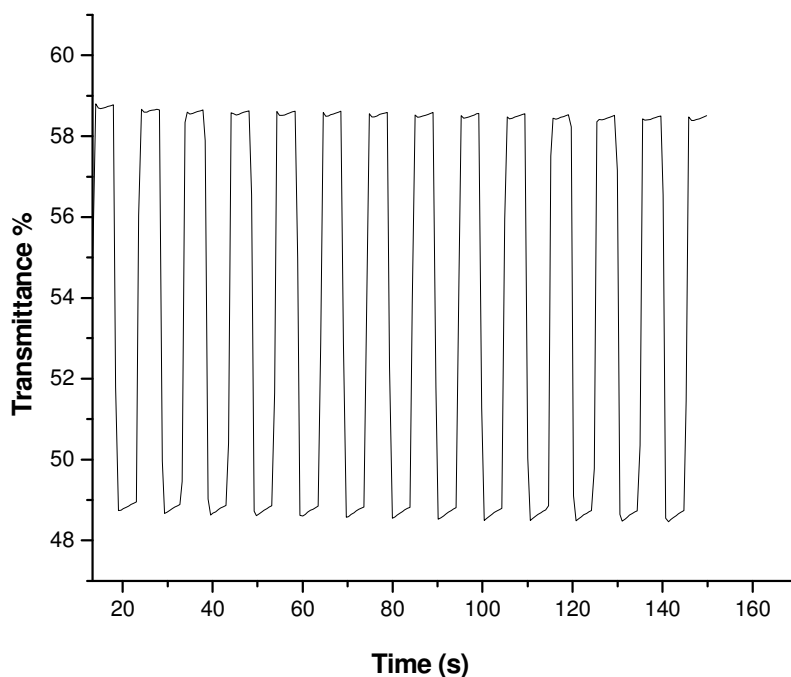


**Figure 3.17** Electrochromic switching, optical absorbance change monitored at 545 nm for P(PTP-co-EDOT)/PEDOT device between -0.8 V and 1.8 V

In order to investigate the electrochromic switching properties of P(PTP-co-EDOT)/PEDOT device, the device was switched between the claret red state in the reduced form ( -0.8 V) and the blue state in the oxidized form (1.8 V) with a residence time of 5 s (Figure 3.17). The device possesses a  $\Delta T$  % of 15% at 545 nm ( $\lambda_{\text{max}}$  for P(PTP-co-EDOT)/PEDOT). It should be noted that the increase of the contrast ratio in P(PTP-co-EDOT)/PEDOT compared to pristine P(PTP)/PEDOT is a result of the modification of main chain polymer

structure and combination of the properties supplied by each monomer. Results showed that time required to reach 95% of ultimate  $\Delta T$  % was 1.9 s for P(PTP-co-EDOT)/PEDOT device.

### 3.8.3. Open Circuit Memory

The ability of an ECD that retains its color and optical density while the current is off, termed as open circuit memory.

In order to investigate open circuit memory of PTP/ PEDOT device, experiments were carried out by polarizing the device in the yellow/blue states by an applied pulse for 1s and then holding at open circuit conditions for 200 s. Simultaneously the optical spectrum as a function of time was recorded (Figure 3.18). When polarized in the blue colored state, initially the device presents 75 % (transmittance %) after 200 s, it changes to 66%. A reasonable optical memory in blue colored state was observed under open circuit conditions. Moreover, PTP/PEDOT device is stable in yellow colored state declared by the insignificant variations in %T.

The color persistence in P(PTP-co-EDOT)/PEDOT was examined by polarizing the device in the fully reduced (claret red)/oxidized(blue) states by an applied pulse (-0.8 V/+1.8V, respectively) for 1 s and then holding at open circuit conditions for 200 s. Figure 3.19 presents the optical spectrum at 545 nm as a function of time at open circuit conditions. When polarized in the blue colored state, initially the device presents 55 % (transmittance %) after 200 s, it changes to 53 %. These results indicate that this system does not reach equilibrium under open circuit conditions at +1.8 V. Moreover the device was stable in claret red colored state (- 0.8 V) indicated by the insignificant variations in T %.

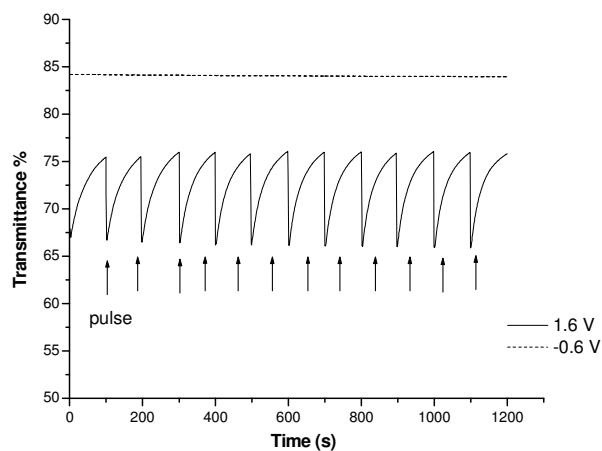


**Figure 3.18** Open circuit memory of P(PTP-co-EDOT)/PEDOT device monitored at -0.6 V and +1.6 V potentials were applied for one second for each 200 seconds time interval at 386 nm

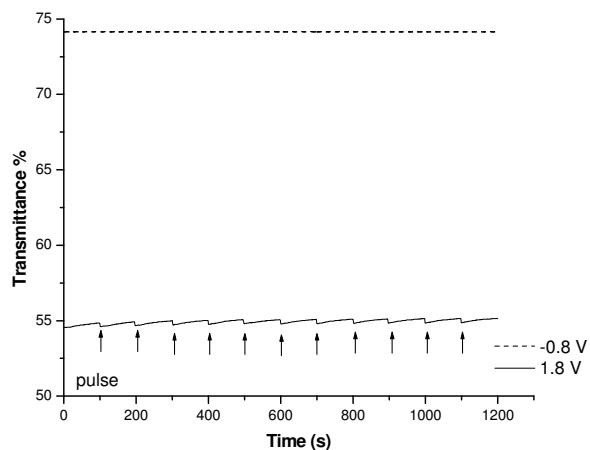


**Figure 3.19** Open circuit memory of P(PTP-co-EDOT)/PEDOT device monitored at -0.8 V and +1.8 V potentials were applied for one second for each 200 seconds time interval at 545 nm

#### 3.8.4. Stability of ECDs

Electrochromic stability is associated with electrochemical stability since the degradation of the active redox couple results in the loss of electrochromic contrast. Therefore, the stability of the device for long term switching between oxidized and neutral states was monitored. Cyclic voltammetry was used to evaluate the stability of the device.

Continuous cycling of the applied potential between -0.6 V and +1.6 V for P(PTP)/PEDOT device with  $500 \text{ mV}\cdot\text{s}^{-1}$  was performed to analyze the stability of device. Figure 3.20 presents the change in the anodic and cathodic peak currents, as a function of the potential. Device showed only a slight decrease in electroactivity accompanied by unperturbed color change from yellow to blue. The device retained 86% of their initial color after 1000 redox cycles. This result revealed that ECD has good environmental and redox stability. Therefore, the device can be operated with applied potentials between -0.6 V and +1.6 V for future applications.

The stability of P(PTP-co-EDOT)/PEDOT device was monitored during continuous cycling of the applied potential between -0.8 V and +1.8 V with  $500 \text{ mV}\cdot\text{s}^{-1}$  under atmospheric conditions. As seen in Figure 3.21, the electrochromic device revealed 10% loss of its electroactivity accompanied by unperturbed color change from bleached to colored state.

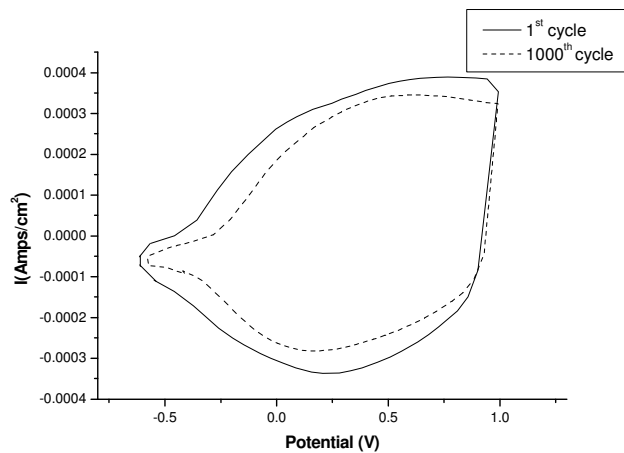


**Figure 3.20** Stability test of P(PTP)/PEDOT device via cyclic voltammetry with a scan rate of  $500 \text{ mV.s}^{-1}$

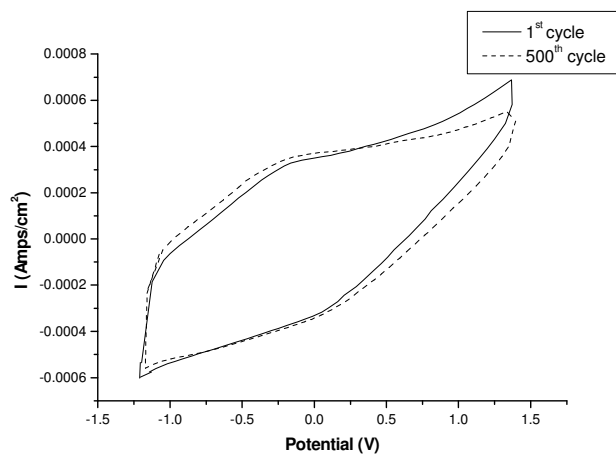


**Figure 3.21** Stability test of P(PTP-co-EDOT)/PEDOT device via cyclic voltammetry with a scan rate of  $500 \text{ mV.s}^{-1}$

## CHAPTER IV

### CONCLUSION

Synthesis of 1-phenyl-2,5-di(2-thienyl)-1*H*-pyrrole (PTP) was successfully accomplished. Polymerization of the monomer was achieved via both chemical and electrochemical methods. As a result of chemical polymerization, a soluble polymer was produced. The structures of both the monomer and the soluble polymer were investigated by  $^1\text{H}$  and  $^{13}\text{C}$ -NMR spectroscopy. Electrochemical synthesis of the conducting homopolymer of PTP was achieved in the presence of ACN/NaClO<sub>4</sub>/LiClO<sub>4</sub> solvent-electrolyte system. As a result, free-standing, stable and electrically conducting polymers were obtained. Investigation of the electrochromic properties of the homopolymer via spectroelectrochemistry and colorimetry and evaluation of its switching ability were also performed. The onset energy for the  $\pi$ - $\pi^*$  transition ( $E_g$ ) was found to be 2.2 eV and  $\lambda_{\text{max}}$  was 413 nm.

A successful synthesis of a conducting copolymer of PTP with EDOT with improved electrochromic properties was achieved. Electrochromic investigations showed that P(PTP) switches between yellow and blue while P(PTP-co-EDOT) was switching between claret red and blue. Color tuning was achieved by changing the conjugation length along the backbone by copolymerization. A profound understanding of these materials' optical properties allowed the construction of electrochromic devices with high contrast, long term switching stability and fast optical response. A P(PTP)/PEDOT device was operated at -0.6 V- 1.6 V, exhibiting an optical contrast of 17 % at  $\lambda_{\text{max}}$ . The device retained 86 % of its initial color after 1000

redox cycles. P(PTP-co-EDOT)/PEDOT device revealed 10% loss of its electroactivity accompanied by unperturbed color change from bleached to colored state after the first 500 cycles.

## REFERENCES

- [1] C. K. Chiang, C. R. Fincher, Jr., Y. W. Park, A. J. Heeger, H. Shirakawa, E. J. Louis, S. C. Gau, and A. G. MacDiarmid, *Phys. Rev. Lett.*, 39 (1977) 1098.
- [2] C. K. Chiang, C. R. Fincher, Jr., Y. W. Park, A. J. Heeger, H. Shirakawa, E. J. Louis, S. C. Gau, and A. G. MacDiarmid, *J. Chem. Phys.*, (1978) 69.
- [3] F. B. Burt, *Journal of Chemical Society*, 68 (1910) 105.
- [4] A. G. MacDiarmid, *Journal of the American Chemical Society*, 98 (1976), 3884.
- [5] H. Letheby, *J. Chem. Soc.*, 15 (1862) 161.
- [6] H. Shirakawa, E. J. Louis, A. G. MacDiarmid, C. K. Chiang, A. J. Heeger, *Journal of Chemical Society- Chemical Communications* (1977) 578.
- [7] R. J. Waltmann, *Can. J. Chem.*, 64 (1986), 76.
- [8] N. Basescu, Z. X. Liu, D. Moses, A. J. Heeger, H. Naarmann, N. Theophilou, *Nature*, 327 (1987) 403.
- [9] H. Naarmann, N. Theophilou, *Synthetic Metals*, 22 (1987) 1.

- [10] J. L. Reddinger, J. R. Reynolds, *Advances in Polymer Science*, 145 (1999), 57.
- [11] H. S. Nalwa, *Handbook of Organic Conductive Molecules and Polymers*, Wiley, New York, 1997.
- [12] T. A. Ed. Skotheim, *Handbook of Conducting Polymers*, Marcel Dekker, New York, (1986), Vol 1 and 2.
- [13] K. Wilbourn, R. W. Murray, *J. Phys. Chem.*, 92 (1988) 3642.
- [14] M. Pomerantz, In *Handbook of Conducting Polymers*; 2<sup>nd</sup> ed.: T. A. Skotheim, R. L. Elsenbaumer, J. R. Reynolds, Ed: Marcel Dekker: New York, (1998)227.
- [15] G. Blasse, B.C. Grabmaier, *Luminescent Materials*, Springer-Verlag (1994).
- [16] K. Shimamura, F. E. Karasz, J. A. Hirsch, J. C. W. Chien, *Makromol Chem Rapid Commun* 2 (1981) 473.
- [17] T. A. Skotheim, J. R. Reynolds, R. L. Elsenbaumer, *Handbook of conducting Polymers*, Marcel Dekker, New York, 1998
- [18] J. L. Bredas, B. Thernans, J. G. Fripiat, J. M. Andre, R. R. Chance, *Synthetic Metals*, 9 (1984) 265.

- [19] J. A. E. H. Van Haare, E. E. Havinga, J. L. Van Donegen, R. A. J. Janssen, J. Cornil, J. L. Bredas, *Chem. Eur. J.*, 4 (1998) 1509.
- [20] J. Tanguay, M. Slama, M. Hoalet, J. L. Baudouin, *Synthetic Metals*, 28 (1989) 145.
- [21] A. G. MacDiarmid, A. J. Heeger, *Synthetic Metals*, 1 (1979) 101.
- [22] M. G. Kanatzidis, *Chem. Eng. News*, 68 (1990) 36.
- [23] A. G. MacDiarmid, *Angew. Chem. Int. Ed.*, 40 (2001) 2581.
- [24] R. Sugimoto, S. Takeda, H.B. Gu, K. Yoshino, *Chem. Express* 1 (1986) 635.
- [25] E. Riande, R. Diaz-Calleja, *Electrical Properties of Polymers*, Marcel Dekker, New York, (2004), Ch.14, 575.
- [26] A. D. Child, J. R. Reynolds, *J. Chem. Soc., Chem. Commun.*, (1991) 1779.
- [27] J. G. Likkian, PhD thesis, The Johns Hopkins University, 2000.
- [28] P. J. Nigrey, A. G. MacDiarmid, and A. J. Heeger, *Chem. Commun.*, 96 (1979) 594.
- [29] R. G. Duan, PhD thesis, University of Minnesota, 1997.

- [30] G. P. Evans, *Advances in Electrochemical Science and Engineering*, Cambridge, 1990, Vol. 1.
- [31] M. E. G. Lyons, *Electroactive Polymer Electrochemistry*, Plenum Press, New York, 1994, Part 1.
- [32] A. N. Samukhin, V. N. Prigodin, L. Jastrabik, A. J. Epstein, *Phys. Rev. B.*, 58 (1998) 11354.
- [33] C. O. Yoon, R. M. D. Moses, A. J. Heeger, Y. Cao, T. A. Chen. X. Wu. R. D. Rieke, *Synthetic Metals*, 75 (1995) 229.
- [34] D. Kumar, R. C. Sharma, *Eur. Poly. J.*, 34 (1998) 1053.
- [35] G. Schopf, G. Kofmehl, *Adv. Polym. Sci.*, 129 (1997) 3.
- [36] R.D. McCullough, *Adv. Mater.*, 10 (1998) 93.
- [37] G. G. Wallace, G. M. Spinks, L. A. P. Kane-Maguire, P. R. Teasdale, *Conductive Electroactive Polymers*, CRC Press, New York, (2003), Ch.2, 51.
- [38] A. Malinauskas, *Polymer* 42 (2001) 3957.
- [39] R. H. Baughman, J. L. Bredas, R.R. Chance, R. L. Elsenbaumer, L. W. Shacklette, *Chem. Rev.*, 82 (1982) 209.
- [40] R. J. Mortimer, A. L. Dyer, J. R. Reynolds, *Displays*, 27 (2006) 2.

- [41] J. Roncali, Chem. Rev., 92 (1992) 711.
- [42] H.S. O. Chan, S. C . Ng, Prog. Polym Sci., 23 (1998) 1167.
- [43] G. Zotti, G. Schiavon, A. Berlin, G. Pagani, Chem. Mater., 5 (1993) 430.
- [44] P. Audebert, P. Hapiot, Synthetic Metal, 75 (1995) 95.
- [45] D. Delabouglés, R. Garreau, M. Lemaire, J. Roncali, New J. Chem., 12 (1988) 155.
- [46] A. R. Hillman, E. Mallen, J Electroanal. Chem., 243 (1998) 403.
- [47] G. Tourillon, F. Garnier, J. Electroanal. Chem. ,135 (1982) 173.
- [48] J. R. Reynolds,S. G. Hsu,H. J. Arnott, j. Polym. Sci. Part B Polym Phys 27 (1989) 2081.
- [49] G. Zotti, Handbook of Organic Conductive Molecules and Polymers, ed. H. S. Nalwa, Wiley, Chichester, 1997, Vol. 2, Ch. 4.
- [50] A. H. Schroeder, F. B. Kaufman, V. Patel, E. M. Engler, J. Electroanal. Chem., 113 (1980) 193.
- [51] T. Johansson, W. Mammo, M. Svensson, M. R. Andersson, o. Inganas, J. Mater. Chem., 13 (2003) 1316.

- [52] J. A. Irvin, J. R. Reynolds, *Polymer* 39 (1998) 2339.
- [53] A. O. Patil, A. J. Heeger, F. Wudl, *Chem. Rev.*, 88 (1988)183.
- [54] A.S. Riberio, W. A. Gazotti Jr. , P. F. S. Filho, M. de Paoli, *Synthetic Metals* 145 (2004) 43.
- [55] F. Jonas, G. Heywang, *Electrochimica Acta*, 39 (1994) 1345.
- [56] B. Krische, M. Zagorzka, *Synthetic Metals*, 28 (1989) 263.
- [57] F. Larmant, J. R. Reynolds, B. A. Reinhardt, L. L. Brott, S. J. Clarson, J. *Polym. Sci : Part A : Polym Chem*, 35 (1997) 3627.
- [58] S. Alkan, L. Toppare, Y. Hepuzer, Y. Yagci, *Synthetic Metals*, 119 (2001) 134.
- [59] W. S. Huang, J. M. Park, *J. Chem. Soc., Chem. Comm.* 1987, 856.
- [60] H. S. Nalwa, *Sythetic Metals*, 35 (1990) 387.
- [61] K. Kaneto, Y. Kohno, K. Yoshino, Y. Inushi, *J. Chem. Soc., Chem. Commun.*, 382 (1983).
- [62] Q. T. Zhang, J. M. Tour, *J. Am Chem. Soc.*, 119 (1997) 5065.

- [63] A. Star, Y. Lu, K. Bradley, G. Gruner, *Nano Lett.* 4 (2004) 1587.
- [64] C. J. Scotl, *Science*, 278 (1997) 2071.
- [65] J. S. Miller, *Adv. Mater.*, 5 (1993)587.
- [66] A. G. MacDiarmid, *Sythetic Metals*, 84(1997)27.
- [67] G. Tourillon, F. Garnier, M. Garzard, j. C. Dubois, *J. Electroanal. Chem.*, 148(1983) 299.
- [68] S. Wang, E. K. Todd, M. Birau, J. Zhang, X. Wan, Z. Y. Wang, *Chem. Mater.* 17 (2005) 6388.
- [69] W. R. Salanecka, R. H. Friend, J. L. Bredas, *Phys. Reports*, 319 (1999) 231.
- [70] O. Tillement, *Solid State Ionics*, 68 (1994) 9.
- [71] D. M. Welsh, PhD., University of Florida,2001.
- [72] C. G. Granqvist, *Electrochim. Acta* 44 (1999) 3005.
- [73] H. Yoneyama,m Y. Shoji, *J. Electrochem. Soc.*, 137 (1990) 3826.

- [74] G. Sönmez, *Chem Commun* 42 (2005) 5251.
- [75] M. Onada, H. Nakayama, S. Morita, K. J. Yoshino, *J Electrochem. Soc.* 141 (1994) 338.
- [76] B. Sankaran, J. R. Reynolds, *Macromolecules*, 30 (1997) 2582.
- [77] P. R. Somani, S. Radhakrishnan, *Mat. Chem. Phys.* 77 (2002) 17.
- [78] G. Sonmez, H. Meng, F. Wudl, *Chem. Mater.* 16 (2004) 574.
- [79] M.A. De Paoli, W. A. Gazotti, *J. Braz. Chem. Soc.*, 13, (2002) 4.
- [80] K. Gurunathan, A.V. Murugan, R. Marimuthu, U.P. Mulik, D.P. Amalnerkar, *Mater. Chem. Phys.* 61 (1999) 173.
- [81] D. M. Welsh, A. Kumar, E. W. Meijer, J. R. Reynolds, *Adv. Mater.*,16 (1999)11.
- [82] A. A. Argun, P.H. Aubert, B. C. Thompson, I. Schwendeman, C. L. Gaupp, J. Hwang, P. Jungseek, J. Nicholas, D. B. Tanner, A. G. MacDiarmid, J. R. Reynolds, *Chem. Mater* 16 (2004) 4401.
- [83] G. Sonmez, C. K. F. Shen, Y. Rubin, F. Wudl, *Angew. Chem. Int. Ed.* 43 (2004)1498.

- [84] B. C. Thompson, P. Schottland, K. Zong, J. R. Reynolds *Chem. Mater.* 2000, 12 (2000) 1563.
- [85] H.J. Kooreman, H. Wynberg, *Rec. Trav. Chim. Pays-Bas.* 86 (1967) 37.
- [86] H. Stetter, B. Rajh, *Chem.* 5 (1968) 454.
- [87] J. Kagan, S.K. Arora, *Heterocycles*, 20 (1983) 1941.
- [88] J. Kagan, S.K. Arora, *Heterocycles*, 20 (1983) 1937.
- [89] H. Wynberg,; J. Metselaar, *Synth. Commun.*, 14 (1984) 1.
- [90] W.Y. Leung, E. Legoff, *Synth. Commun.*, 19 (1989) 787.
- [91] A. Merz, F. Ellinger, *Synthesis*, 6 (1991) 463.
- [92] L.H. Chen,; C.Y. Wang, T.M. H. Luo, *Heterocycles*, 38 (1994) 1393.
- [93] I. Schwendeman, PhD. Thesis, University of Florida, 2002.
- [94] O. C. Wells, *Scanning Electron Microscopy*, MacGraw-Hill Publishing, New York, (1974),2.